

Spring 5-10-2019

Process Optimization of Levulinic Acid Production From Seaweeds and Its Upgrading to TDO Oil

Maurvin Patel

University of Maine, maurvin.patel@maine.edu

Follow this and additional works at: <https://digitalcommons.library.umaine.edu/etd>

 Part of the [Civil Engineering Commons](#)

Recommended Citation

Patel, Maurvin, "Process Optimization of Levulinic Acid Production From Seaweeds and Its Upgrading to TDO Oil" (2019).
Electronic Theses and Dissertations. 3008.
<https://digitalcommons.library.umaine.edu/etd/3008>

This Open-Access Thesis is brought to you for free and open access by DigitalCommons@UMaine. It has been accepted for inclusion in Electronic Theses and Dissertations by an authorized administrator of DigitalCommons@UMaine. For more information, please contact um.library.technical.services@maine.edu.

**PROCESS OPTIMIZATION OF LEVULINIC ACID PRODUCTION FROM
SEAWEEDS AND ITS UPGRADING TO TDO OIL**

By

Maurvin Patel

B.S Pandit Deendayal Petroleum University, 2015

A THESIS

Submitted in Partial Fulfillment of the

Requirements for the Degree of

Masters of Science

(in Chemical Engineering)

The Graduate School

The University of Maine

May 2019

Advisory Committee:

Dr. Peter Van Walsum, Associate Professor of Chemical Engineering, Advisor

Dr. M. Clayton Wheeler, Professor of Chemical Engineering

Dr. Adriaan Van Heiningen, Professor of Chemical Engineering

PROCESS OPTIMIZATION OF LEVULINIC ACID PRODUCTION FROM SEAWEEDS AND ITS UPGRADING TO TDO OIL

By Maurvin Patel

Thesis Advisor: Dr. Peter Van Walsum

An Abstract of the Thesis Presented
in Partial Fulfillment of the Requirements for the
Degree of Masters of Science
(in Chemical Engineering)

May 2019

ABSTRACT

Levulinic acid (LA) is a platform chemical and it can be upgraded to various products like bio-oil. The acid hydrolysis of cellulose is a widely researched pathway to make LA. However, investments to produce LA commercially can be subjected to risks due to feedstock price volatility and high processing costs. Such risks can be reduced by expanding the feedstock portfolio to produce LA from feedstock beyond wood and improving the energy efficiency of the process.

One little investigated feedstock for production of LA is macro algae (seaweed). Seaweed is potentially attractive because it has low content of lignin or 5 carbon carbohydrates, which complicate production of LA. In this study, we investigated the production of LA from sugar kelp (Brown Seaweed) via two-stage and three stage sulfuric acid hydrolysis in a batch process. The highest of yield of levulinic acid for two stage hydrolysis was noted as 30.11 mol% (theoretical yield on available glucan) obtained at 200 °C with 120 min retention time. Three stage hydrolysis produces around 28 mol% at 200 °C with 80 min retention time with 4 (% wt) H₂SO₄.

LA can be upgraded to bio-oil using the Thermal Deoxygenation (TDO) pathway. The production of TDO oil from woody biomass derived LA is found to be an energy intensive process. So, energy integration is helpful to minimize overall energy consumption of the renewable fuel production, which eventually reduces the cost of fuel production. We performed energy integration analysis of the combined AHDH and TDO process using the pinch analysis methodology to determine potential energy savings. The combined AHDH and TDO pathway includes: evaporation loads, condensation heat duties, exothermic reaction duties and more efficient use of utility systems. The energy integration analysis is divided into three major tasks: (i) selection of matches, (ii) minimum utility cost estimation, and (iii) determining minimum cost of heat exchanger network. The calculation of the Pinch Point done by theoretical and graphical methods yielded 107 °C and 97 °C for hot and cold streams, respectively. The energy savings of the combined AHDH and TDO pathway to make renewable fuel was evaluated by using data collected from Aspen Plus. The potential energy saving was calculated to be 94.40 MW, which is around 59% of total steam demand. The installation cost of heat exchangers with energy integration is found to be higher, but only moderately so, compared to the process of without energy integration. Overall the total cost savings is estimated to be around 50% reduction of combined utility and capital costs for the heat exchanger network. This improves the overall economic performance of combined AHDH and TDO pathway to make renewable fuel. Thus, the prime objective of energy integration was achieved by increasing process to process heat transfer and by reducing extra utility loads.

ACKNOWLEDGEMENTS

I would like to express my immense gratitude to my advisor Dr. Peter Van Walsum for his dedication, hard work, support, and knowledge throughout my research. I would also like to thank Dr. Adriaan R. P. van Heiningen for allowing me to use his laboratory instruments.

I wish to extend my thanks to my committee member Dr. Clayton Wheeler for his valuable time and support. I am grateful to Dr. Sampath Reddy Gunukula for his guidance and support. Thanks to Dr. Ravikant Patil for training and support with analytical instruments. In addition, I'd like to thank Praveen Sappati for helping with multiway ANOVA and Amos Cline for his technical support.

I would also like to recognize National Science Foundation projects: Sustainable Energy Program and Sustainable Ecological Aquaculture Network (SEANET) for contributing funding and materials to this research. I am grateful to Dr. Hemant Pendse for providing financial support through the department of Chemical and Biomedical Engineering and the Forest Bioproducts Research Institute (FBRI), as well.

Finally, I am grateful to my family and friends for their support, love and friendship.

TABLE OF CONTENTS

ACKNOWLEDGEMENTS	ii
TABLE OF CONTENTS.....	iii
LIST OF TABLES	vii
LIST OF FIGURES	ix
LIST OF EQUATIONS	x
CHAPTER 1	1
1.1 Introduction	1
1.1.1 Conversion of Biomass to Levulinic acid.....	6
1.2 Materials and Methods	13
1.2.1 Apparatus and Chemicals	13
1.2.1.1 Apparatus	13
1.2.1.2 Reagents.....	14
1.2.1.3 Materials	14
1.2.2 Sample Preparation.....	15
1.2.3 Physiochemical Analysis.....	15
1.2.3.1 Moisture Content	15
1.2.3.2 Ash Content:	16
1.2.3.3 Protein Content:	17
1.2.3.4 Lipid Content and carbohydrate content:.....	17
1.2.4 Sugar Analysis of Sugar Kelp	17
1.2.5 Acid Hydrolysis of Sugar Kelp at High Temperature	18

1.2.6 Three Stage Hydrolysis of Sugar Kelp	19
1.2.7 Acid Hydrolysis of Pure Individual Carbohydrates	19
1.2.8 Analytical Methods.....	20
1.2.9 Statistical Analysis	22
1.3 Results and Discussion.....	22
1.3.1 Moisture Content	22
1.3.2 Ash Content	22
1.3.3 Fat Content	23
1.3.4 Protein Content.....	23
1.3.5 Carbohydrate Content.....	23
1.3.6 Sugar Analysis of Seaweed	26
1.3.7 AHDH of Sugar Kelp at High Temperature (two stage acid hydrolysis).....	27
1.3.8 Three Stage Hydrolysis and Dehydration of Sugar Kelp	28
1.4 Conclusion.....	39
CHAPTER 2	41
2.1 Introduction	41
2.1.1 Process Description of Bio-fine process and Thermal Deoxygenation	43
2.2 Materials and Methods	45
2.2.1 Data Extraction or Stream Table	45
2.2.2 Composite Curve/Temperature -Enthalpy Diagram.....	46
2.3.3 Grand Composite Curve	47
2.2.3 Grand Composite Curve (Residual heat curve).....	50

2.2.4 Placing of Heat Exchangers.....	51
2.2.5 Area Targeting/Heat Exchanger Network	53
2.2.6 Calculation of Heat Exchanger Area in ASPEN Plus	54
2.2.7 Cost Estimation.....	54
2.2.7.1 Utility Cost Calculation	54
2.2.7.2 Installed Cost Calculation	55
2.2.7.3 Capital Cost of Estimation.....	56
2.2.7.4 Total Annualized Cost	56
2.3 Results and Discussion.....	57
2.3.1 Data Extraction.....	57
2.3.2 Composite Curve	59
2.3.4 Area Targeting Network.....	62
2.3.5 Cost Targeting	66
2.3.6 Capital Cost of Heat Exchangers.....	66
2.3.7 Operating Cost of Heat Exchangers	68
2.3.8 Total Cost of Heat Exchangers.....	69
2.4 Conclusion.....	70
BIBLIOGRAPHY.....	71
APPENDIX A MASS BALANCE CALCULATIONS	78
APPENDIX B SUGAR ANALYSIS AND LEVULINIC ACID ANALYSIS OF SUGAR KELP.....	79

APPENDIX C UTILITY COST OF THE PROCESS WITH AND WITHOUT ENERGY

INTEGRATION 83

BIOGRAPHY 85

LIST OF TABLES

Table 1 Biomass Feedstock and Reaction Conditions for the Production of Levulinic Acid	8
Table 2 Physiochemical results of Seaweed on dry basis.....	22
Table 3 Sugar Analysis Results of Sugar Kelp.....	30
Table 4 Levulinic Acid as a Byproduct from Sugar Analysis of Sugar Kelp.....	30
Table 5 Levulinic Acid Results from Two Stage Acid Hydrolysis (based on mol%)	31
Table 6 Levulinic Acid Results from Two Stage Acid Hydrolysis (based on mass%)	32
Table 7 Levulinic Acid Results for Three Stage Acid Hydrolysis (based on mol%)	33
Table 8 Levulinic Acid Results for Three Stage Acid Hydrolysis (base on mass%)	34
Table 9 Levulinic Acid Results from Two Stage Acid Hydrolysis (based on Carbohydrate 48.5%).....	35
Table 10 Levulinic Acid Results for Three Stage Acid Hydrolysis (based on carbohydrate percentage).....	36
Table 11 Acid Hydrolysis of Individual Carbohydrates.....	37
Table 12 Data Extraction for Energy Integration	58
Table 13 Cumulative Heat Duty of Hot Streams and Cold Streams in Temperature Intervals	60
Table 14 Table for Grand Composite Curve.....	61
Table 15 Stream Matching and Heat Exchanger Area.....	65
Table 16 Purchased and Installed Costs of Heat Exchangers	67
Table 17 Annual Utility Costs (Operating days per year:330)	69
Table 18 Cost Comparison of Heat Exchangers	69
Table 19 Sugar Analysis Results of Sugar Kelp.....	79
Table 20 Levulinic Acid as a Byproduct from Sugar Analysis of Sugar Kelp.....	79

Table 21 Results of Levulinic acid from Two Stage Hydrolysis (with 4% H ₂ SO ₄).....	80
Table 22 Results of Levulinic acid from Two Stage Hydrolysis (with 6 wt% H ₂ SO ₄).....	80
Table 23 Results of Levulinic Acid from Two Stage Hydrolysis (with 8 wt% H ₂ SO ₄).....	81
Table 24 Results of Levulinic Acid from Three Stage Hydrolysis (with 4 wt% H ₂ SO ₄).....	81
Table 25 Results of Levulinic Acid from Three Stage Hydrolysis (with 6 wt% H ₂ SO ₄).....	82
Table 26 Results of Levulinic Acid from Three Stage Hydrolysis (with 8 wt% H ₂ SO ₄).....	82
Table 27 Annual Cost of Utility with their Coefficients (Process with energy Integration)	83
Table 28 Annual Cost of Utility with their Coefficients (Process w/o energy Integration)	83
Table 29 HPAEC Results for Sugar Analysis Results of Sugar Kelp	84

LIST OF FIGURES

Figure 1 Transformation of Levulinic acid into value added chemicals and biofuels (21)	7
Figure 2 Conversion Pathways of Cellulose into Levulinic acid (19).....	7
Figure 3 Continuous process for the production of LA from hexose yielding material based on Dunlop et al., (1957) (39)	10
Figure 4 Process flow diagram for extrusion process based on description by Ghorpade et al., (1999) (40).....	11
Figure 5 Process flow diagram for Production of LA from bio fine process (41).....	12
Figure 6 Alginate Structure.....	24
Figure 7 Chemical structure of Mannitol.....	25
Figure 8 Linear Structure of cellulose	25
Figure 9 Possible Laminarin Structure with D-Mannitol (M-chain) Residues at the end (58).....	26
Figure 10 Possible Laminarin Structure with D-glucose (G-chain) Residues at the end (58).....	26
Figure 11 Acid catalyzed pathway of cellulose to Levulinic acid	28
Figure 12 Acid hydrolysis pathway from conversion of glucose to levulinic acid	29
Figure 13 Block Flow Diagram of Combined AHDH and TDO Oil (6)	44
Figure 14 Grand Composite Curve	48
Figure 15 Net Energy Requirement in Each Interval.....	49
Figure 16 Algorithm for Matching of Streams Above Pinch Region.....	52
Figure 17 Algorithm for Matching of Streams Below Pinch Region	52
Figure 18 Composite Curve	62
Figure 19 Balanced Composite Curve	62
Figure 20 Complete Minimum Energy Design.....	64

LIST OF EQUATIONS

Equation 1 % Ash	16
Equation 2 % of Protein	17
Equation 3 Net energy balance in each interval.....	46
Equation 4 Net energy balance in each interval factoring in Q_{latent}	47
Equation 5 Cumulative heat duty for sensible heat	50
Equation 6 Cumulative heat duty for sensible heat factoring in Q_{latent}	50
Equation 7 Sensible heat streams left-over energy	51
Equation 8 Overall heat transfer area.....	53
Equation 9 Log mean temperature difference.....	53
Equation 10 Utility Cost	54
Equation 11 Price of tap water.....	55
Equation 12 Installed cost of heat exchanger in 2016	56
Equation 13 Annualized capital cost.....	56
Equation 14 Theoretical yield of glucose (mmol)	78
Equation 15 % of glucose yield (based on glucan content)	78
Equation 16 % of theoretical yield of levulinic acid (based on glucan content)	78
Equation 17 % of levulinic acid yield (based on glucan content).....	78
Equation 18 % yield of levulinic acid (mol%).....	78
Equation 19 % yield of levulinic acid (% wt).....	78

CHAPTER 1

1.1 Introduction

Currently most fuels and chemicals are made from non-renewable fossil feedstock such as crude oil, natural gas or coal. The International Energy Agency reported around 81% of total energy production was associated with fossil fuels and 90% of total transportation fuels were derived from petroleum based feedstock (1). An increasing global population and continuing industrialization increase the global energy demand. The U.N. department of economics and affairs projects the global population to be around 9 billion by 2050 (16). However, fossil fuels are non-renewable energy sources and problems associated with petroleum based feedstock, such as greenhouse gas emissions (the global carbon emission was 32.5 gigatonnes in 2017), depletion of oil reserves and climate change give a new direction to research to find an alternative source of energy and fuels. The environmental impacts of fossil fuels can be reduced with the utilization of renewable biomass such as wood and corn Stover. Biofuels such as ethanol and biodiesel can be produced from biomass. Currently they are blended with gasoline and diesel to use for transportation fuels, which results in life cycle greenhouse gas emission reduction (3). In 2005, United States proposed the renewable fuel standard under the Energy Policy Act (EPA act), requiring 24 billion gallons of renewable fuel to be blended with gasoline, the goal of this project was to increase the volume of renewable fuels to 36 billion gallons by 2022 (3).

Lignocellulosic biomass is the most abundantly available raw material, with worldwide availability of around 450 billion dry tones of biomass as a potential source of energy (2). There are several currently proposed technologies to upgrade lignocellulosic biomass to fuels and chemicals. These technologies are categorized as: thermochemical, catalytic, and biological technologies. Thermochemical technologies involve heating of biomass in the presence or in the

absence of a catalyst to make fuels and chemicals. Pyrolysis, combustion, and gasification, are examples of thermochemical pathways (4). Pyrolysis is the process to convert biomass into liquid, char and gases at different temperature ranges between 300 °C to 700 °C in the absence of air. Slow pyrolysis and fast pyrolysis are the types of pyrolysis processes. Slow pyrolysis converts biomass into valuable products in a slow heating rate, and the main product of this process is char along with small amounts of bio oil and gases (5). Fast pyrolysis takes place in a moderate to high temperature range to convert biomass into organic vapors, char and gases within a small residence time of anywhere between 2 and 10 sec. But a problem associated with the fast pyrolysis is high oxygen content in the resulting oil which causes the oil to be unstable. A hydro treating process can be used to upgrade bio-oil by removing oxygen of bio-oil to make hydrocarbon fuel. Three catalytic steps with severe conditions are necessary to remove the oxygen. Catalytic deactivation due to the formation of coke during the hydro treating process is the main concern for the commercialization of transportation fuel production via this process (9). Catalytic fast pyrolysis is the process to produce the bio-oil in a fast pyrolysis reactor assisted with in-situ catalyst (6). Zeolite (ZSM-5) can be used at atmospheric pressure without hydrogen to promote the cracking reaction to increase the C/O ratio and aromatic concentration in bio-oil (7). Combustion is a burning of biomass at very high temperature (800 °C to 1000 °C) in air to convert the energy stored in biomass to mechanical power or electricity using various equipment. This process is useful for small scale household purposes such as cooking as well as generation of electricity in an industrial level (4). Gasification is a conversion of biomass into combustible gases or synthesis gases at the temperature range of 800 to 900 °C in the presence of limited amounts of air or steam. The resulting synthesis gases can be used to produce chemicals. Combustible gases can be useful to run gas turbine or gas engines. The idea behind biomass gasification is to convert gaseous fuel

into electricity by using a gas turbine, which increases the efficiency of the process (4). Hydrothermal Liquefaction is a thermochemical route for production from dry and/or wet biomass in the presence of catalyst along with hydrogen at moderate temperature condition (280-370 °C) (10). The product in this process stream contains gases, aqueous components, and solids along with the main product as liquid. This process takes place at high pressure (10-25 MPa) to increase the heat recovery. Feeding the system at these high temperatures and the high pressure rating on the reactor are concerns that make this process less attractive (11).

Ethanol can be produced from lignocellulosic biomass via the biological pathway. The biological pathway is characterized by slow reaction rates and lower temperature conditions, and it is suitable for high moisture content feedstock. The process includes bacteria, microorganisms and enzymes that breakdown biomass into carbohydrates and sugars, which are then further converted into fuels and chemicals. Anaerobic digestion and fermentation are examples of biological pathways. Anaerobic digestion is the degradation process to convert wet, organic waste made of biodegradable material such as municipal solid waste, industrial waste, and food waste into biogas. This process takes place in the absence of air. Biogas produced from anaerobic digestion can be used to produce electricity and some transportation fuels. The combined enzymatic hydrolysis and fermentation is an example of a biological pathway that produces fermentable sugars followed by ethanol from a lignocellulosic feedstock.

A wide range of biomass feedstocks have been tested to produce liquid fuels and chemicals. In the US, it is predominantly corn-derived starch that is currently used to make biofuels and chemicals. However, the use of edible feedstock like corn- based starch impacts feed prices. Thus, inedible feedstocks like lignocellulosic feedstock have been explored to make chemicals and fuels. Despite its abundance, the cost of lignocellulosic feedstock can be limiting to the commercialization of

biomass upgrading technologies. To overcome the cost barriers, significant research has been directed at reducing the cost of the processing methods used to convert the feedstock into various chemicals and fuels.

Algae is a diverse group of biomass that grow in aqueous environments. Marine algae are divided into two different groups based on their sizes: (1) Microalgae (unicellular) and (2) Macro algae (multicellular). Researchers have been driving towards the production of biofuels from algae because of its several advantages over lignocellulosic biomass. One advantage is the low content or absence of lignin in algae, which simplifies biofuel processes that are affected by the physical handling and chemical interference issues associated with processing lignin. The presence of lignin in lignocellulosic biomass creates problems in enzymatic hydrolysis processes, so various pretreatment methods such as steam explosion, ammonia fiber expansion, or ionic liquid pretreatment have been applied to make the hydrolysis process easier. A disadvantage of seaweed biomass is a glucan content that is quite low compared to lignocellulosic biomass, although other carbohydrate chemical content such as mannitol, alginate, agar and carrageenan increase the yield of sugar concentrations which can be converted into various chemicals and fuels via thermochemical and bio-chemical pathways subject to the moisture content of biomass. The conversion technologies for dry algae include direct combustion, pyrolysis, gasification and transesterification of extracted oils to biodiesel, whereas hydrothermal treatment and other biochemical treatments such as anaerobic digestion and fermentation can be used to convert wet algae (13). The main concern with dry biomass is that it requires extra steps for drying which makes process more complex and energy consuming. As discussed earlier, direct combustion of seaweed is a traditional method to produce heat and electricity in households or at an industrial level from burning. But the problem associated in this process is the presence of high amounts of

inorganic solid residue such as ash and alkaline content which decreases the process efficiency. Pyrolysis is another thermochemical technology to convert dry algae into biofuels. But in this process, presence of metals and ash cause catalyst deactivation. Gasification takes place at high temperatures, with partial oxidation so that organic materials convert into syngas, which can be further converted into methanol and hydrogen for transportation fuels, but the process is not cost effective. Anaerobic digestion is a suitable biochemical method because of higher energy content and lower greenhouse gas emission. Thermochemical processes are good for lignocellulosic feedstock like wood and biological treatment is preferred for herbaceous feedstock. Moreover, product selectivity also decides the type of biofuel pathway. Butanol production is more towards biological conversion whereas, hydrocarbon fuel production seems more selective towards thermochemical pathways (14). But research shows that oil derived from algae has lower oxygen content, lower viscosity and higher heating value compared to woody biomass; however, the yield of bio-oil derived from algae biomass is quite low compared to woody biomass because of the high ash content and presence of metal contents which tends to lower the acidity of the mixture (47). The problem associated with the presence of ash and inorganic compounds can be solved by using acid hydrolysis at higher sulfuric acid concentration which results in higher fatty acid components into bio-oil but the formation of large char also affects the continuous pyrolysis of macro algae (13). The biochemical pathway is another option for the production of biofuels from algae biomass. Research suggests that anaerobic digestion is more preferable than the thermochemical pathways at an industrial level because it can undergo in the presence of moisture and it has the potential to utilize the entire carbon content of macro algae (13). One problem is that the metal content of algae is released into fermentation products and this could create some

problems in the fermentation, so pretreatment with activated charcoal and lime may be necessary to decrease the metal content (15)

In this study, we are hydrolyzing the brown seaweed *Saccharina latissima*, also known as *Laminaria saccharina*, in a batch reactor to produce levulinic and formic acids through acid hydrolysis and dehydration and optimizing the process for different combinations of temperature, time and acid concentration. The temperature range explored for this process was 150 °C to 200 °C with residence time ranging from 40 minutes to 120 minutes. The range of H₂SO₄ acid concentration was from 2% to 10 % (m/v). Two stage hydrolysis was performed to determine total glucose and other carbohydrate composition in the samples, with different residence times applied at the second stage of hydrolysis to optimize glucose yield. Elemental analysis was done to determine the wt% of nitrogen and carbon. HPLC was performed for quantitative analysis of hydrolyzed seaweed. HPAEC was performed to compare the results of sugar analysis with HPLC analysis.

1.1.1 Conversion of Biomass to Levulinic acid

The Department of Energy reported 12 top value added platform to accelerate the growth of bio based economy. Levulinic acid is one of these twelve promising value added platform chemicals because of its high reactive carbonyl and carboxyl groups that can convert into various value added chemicals by undergoing various chemical reactions (20). Some of the various applications of levulinic acid include: pharmaceutical, plasticizers, food and flavors, solvents, personal care, biodiesel, resins and coatings, herbicides, specialty chemicals, fuel extenders (18).

Figure 1 shows the transformation of levulinic acid into various chemicals and biofuels. The common method for the production of levulinic acid is acid hydrolysis of saccharides at different temperature and pressure conditions via the intermediate 5-hydroxymethylfurfural.

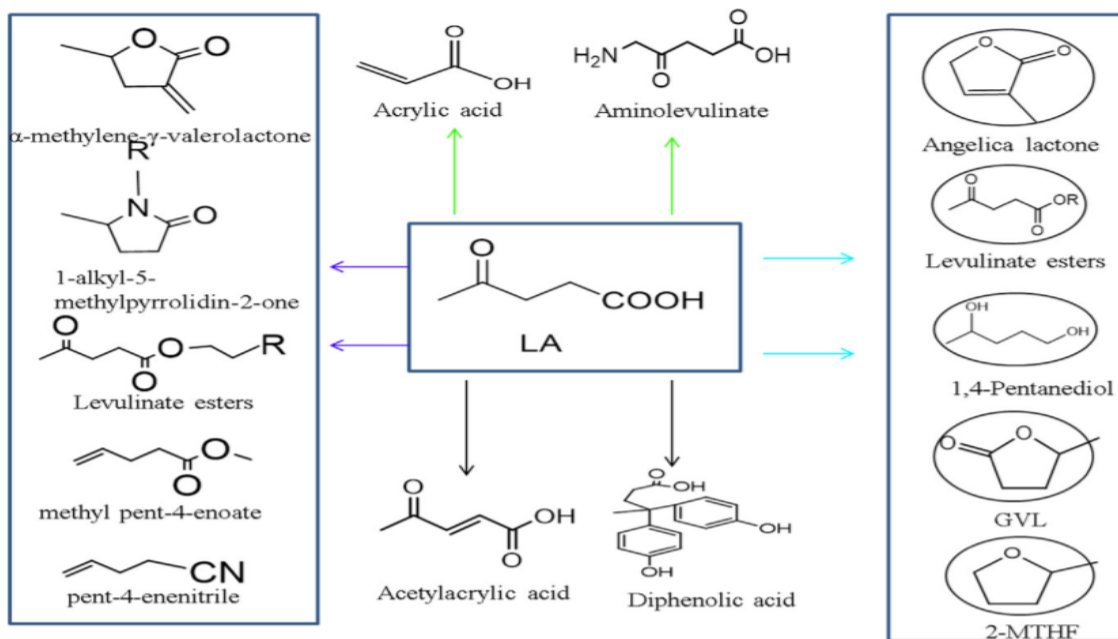


Figure 1 Transformation of Levulinic acid into value added chemicals and biofuels (21)

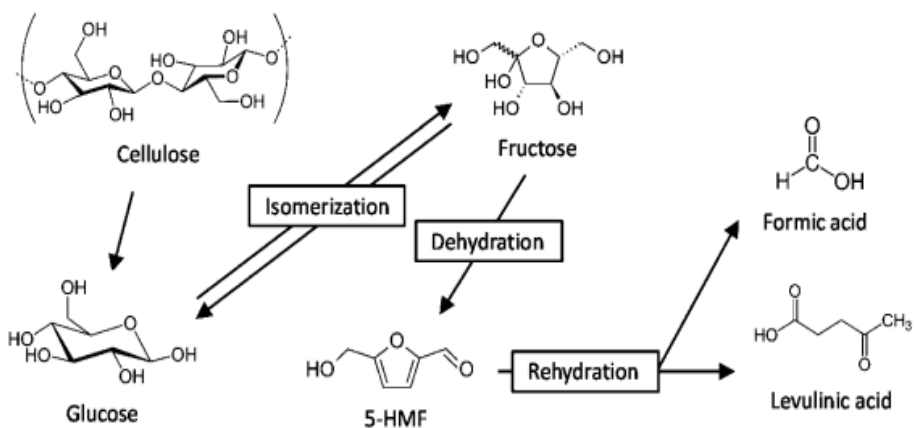


Figure 2 Conversion Pathways of Cellulose into Levulinic acid (19)

Table 1 summarizes results of different studies on conversion of carbohydrate and biomass feedstock to levulinic acid. All the studies presented in the table were carried out in batch process at laboratory scale.

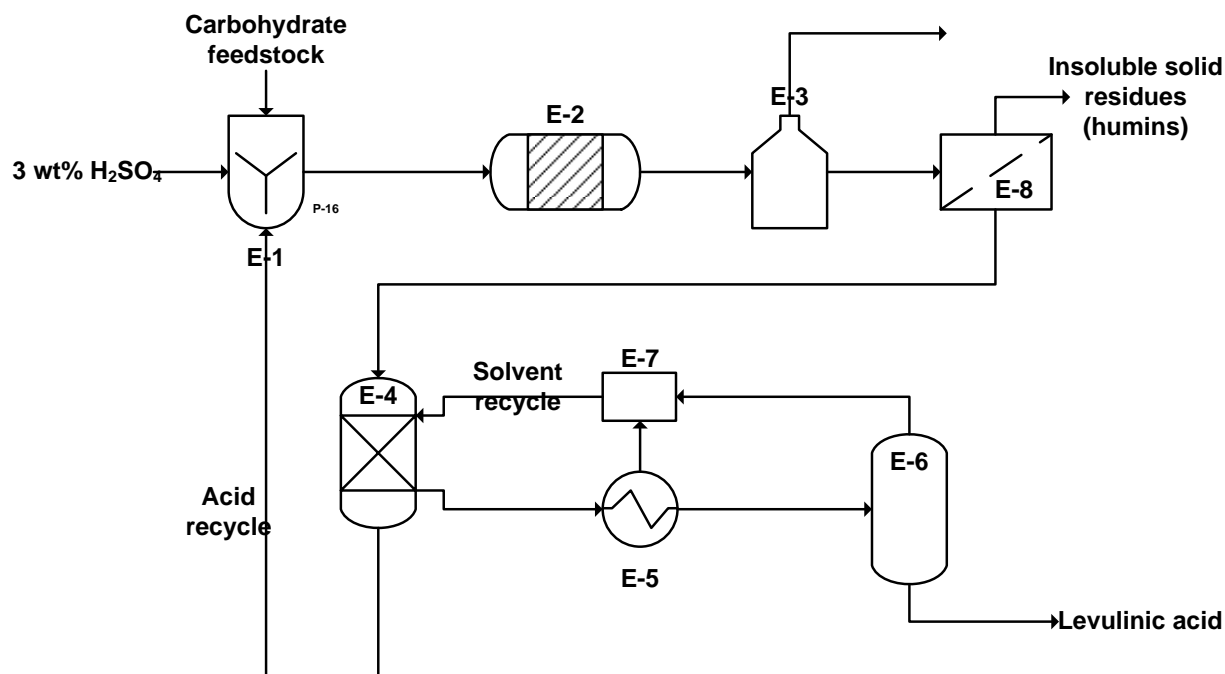
Table 1 Biomass Feedstock and Reaction Conditions for the Production of Levulinic Acid

Feedstock	Feedstock (wt%)	Catalyst	C _{catalyst} (wt%) ^a	T (°C)	t (h)	Y _{LA} (wt%) ^b	Ref
Wheat straw	6.4	H ₂ SO ₄	3.5	210	0.63	19.8	19
Cane sugar	28	HCl	18	100	24	15	22
Glucose	29	HCl	6.5	162	1	24	24
Glucose	n.a.	FeCl ₃	n.a.	180	2	30	25
Glucose	10	HCl	6	160	0.25	41.4	26
Glucose	10	H ₂ SO ₄	n.a.	170-210	1	50.2	27
Cellulose	10	H ₂ SO ₄	3	250	2	25.2	30
Glucose	n.a.	HCl	n.a.	90	4	23	27
Fructose	5-20	HCl	n.a.	98	n.a.	75	27
Fructose	5-10	H ₃ PO ₄	n.a.	280	0.03	7	28
Glucose	27	Amberlite IR-120	19	R.T.	124	5.8	29
Glucose	12	HY-zeolite	3	150	24	6	31
Sucrose	6	HCl	9.7	125	16	43	32
Cellulose	n.a.	H ₂ SO ₄	5-10	150	2	60	33
Cellulose	10	H ₂ SO ₄	1-5	150-250	2-7	25.2	34
Cellulose	10	HCl	1-5	150-250	2-7	28.8	34
Cellulose	10	HBr	1-5	150-250	2-7	26.9	34
Cellulose	10	H ₂ SO ₄	5	150	6	57	35
α-cellulose	n.a.	HCl	n.a.	220	1	45.2	36
Corn Stover	n.a.	HCl	n.a.	80-100	3	5-9	37
Bagasse	9	HCl	4.45	220	0.75	22.8	38
Paddy straw	n.a.	HCl	4.45	220	0.75	23.7	38

^aC_{catalyst}= concentration of catalyst; R.T.= Refluxed temperature; ^bY_{LA}= the ratio of mass of

Levulinic acid and mass of feedstock; n.a.= data is not available

However, there has also been progress in larger scale processes for the production of Levulinic acid (LA) in a continuous process at an industrial level. In 1957, Dunlop and Wells proposed a continuous process for the production of LA from hexose yielding materials at atmospheric pressure. In this process, 21 wt% carbohydrate feedstock (residues from furfural production) was mixed with 3% H₂SO₄. The mixture was passed through a reactor at 169 °C (the temperature range: 150 °C – 200 °C) with a residence time of 3 hours. After the reaction, the products were passed to a filter unit for the separation of insoluble solid residue from product stream. Following this, in a separation unit, methyl isobutyl ketone (selective towards LA) was used as a solvent for the extraction of LA from the aqueous phase. The aqueous phase and catalyst was recycled to the reaction zone. The extraction solvent was purified from an evaporator and LA was sent to vacuum distillation for further purification. With this process. The optimum yield of LA was 19.9 wt% based on dry feedstock (39). The process flow diagram for this method is shown in Figure 3.



E-1: Pre mixer	E-6: LA fractionator
E-2: Reactor	E-7: Solvent recovery
E-3: Flash tank	E-8: Filter unit
E-4: Solvent extraction column	
E-5: Solvent Evaporator	

Figure 3 Continuous process for the production of LA from hexose yielding material based on Dunlop et al., (1957) (39)

Ghorpade and Hanna introduced the concept of extrusion for the production of Levulinic acid (1999). The extrusion process appears to be an efficient process thanks to high process yield combined with low energy and time requirements. In this process, corn starch and 5% H_2SO_4 are mixed in a pre-conditioner to create the slurry of corn starch. In the following step, the slurry of corn starch passes through twin screw extruder with different temperature profiles, such as 80-100 °C, 120-150 °C or 150 °C. After this reaction, the product stream containing levulinic acid passes through a filter press

in which humins are separated from levulinic acid and the remaining mixture is sent to vacuum distillation to increase the purity of levulinic acid. By feeding 820 kg/h of corn starch feedstock, 40 kg/h of 5 wt% H₂SO₄ and 290 kg/h of water yielded the levulinic acid about 48 wt% (40).

The process is shown in Figure 4.

:

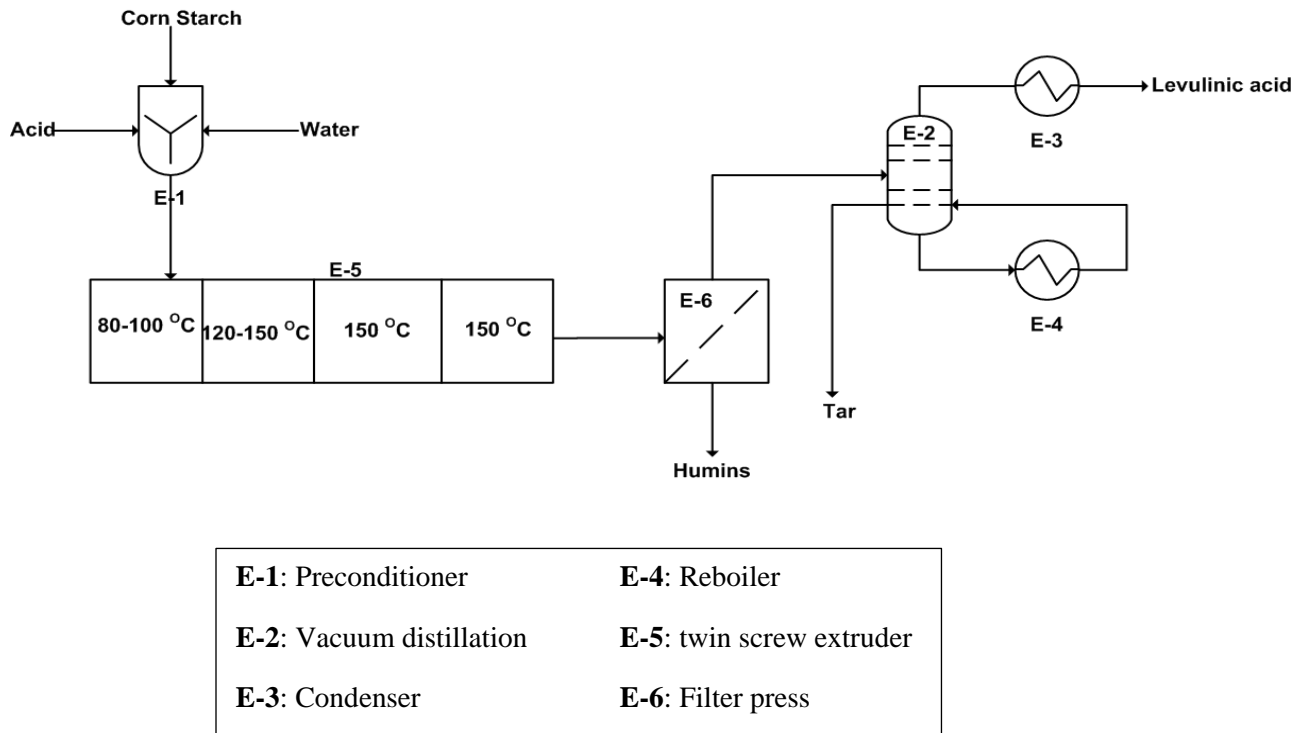


Figure 4 Process flow diagram for extrusion process based on description by Ghorpade et al., (1999) (40)

Bio fine technology is another process for the continuous production of LA by using carbohydrate feedstock. The typical yield of LA from this process is about 60 wt% to 70 wt % of theoretical yield. In this process, dilute H₂SO₄ (1% to 5%) is used as a catalyst and is mixed with carbohydrate feedstock. The slurry of carbohydrate mixture and catalyst is sent to a Plug

Flow Reactor with 12 second residence time at temperature of 210-230 °C which converts all polysaccharides into monosaccharides. The product stream of monosaccharides is transferred into CSTR (Continuous Stirred tank reactor) at 195-215 °C for 15 minutes to 30 minutes to produce LA. The product stream from the CSTR contains vapors of FA (Formic acid), furfural and other products which can be condensed and LA is separated as a liquid from second reactor. Solid by products can be separated from filter press (41).

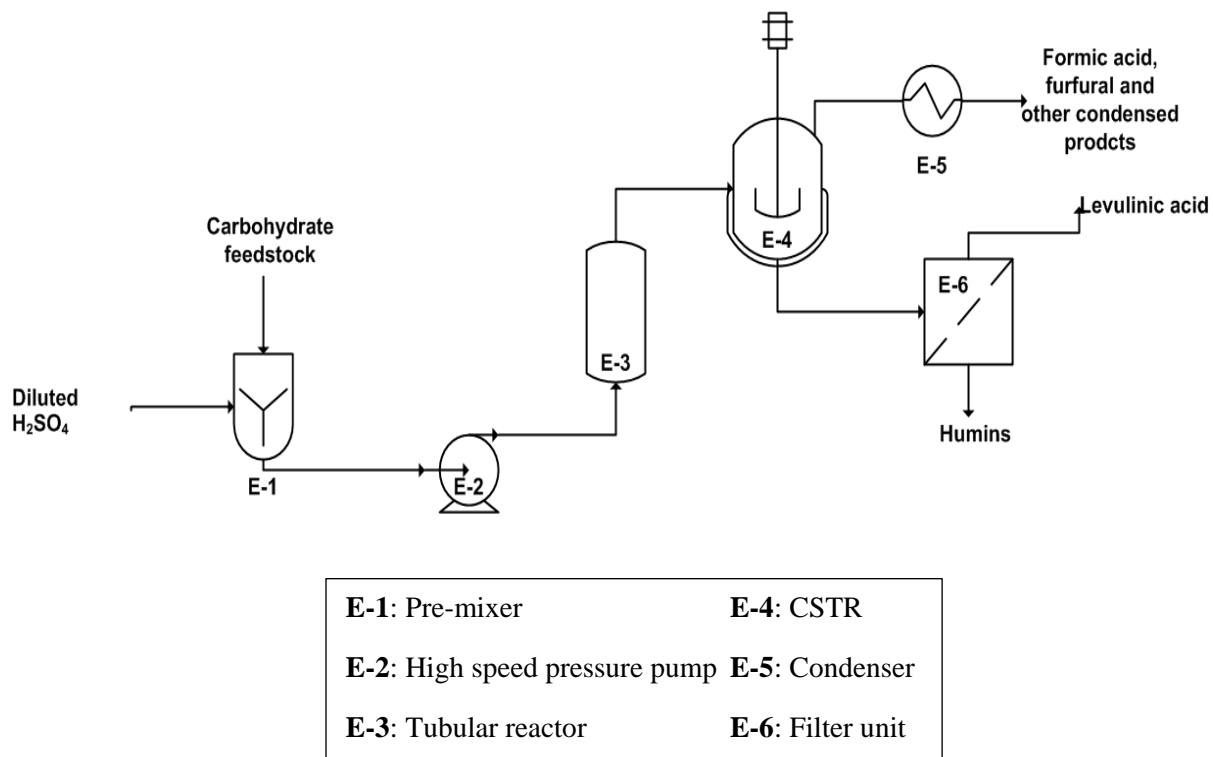


Figure 5 Process flow diagram for Production of LA from bio fine process (41)

1.2 Materials and Methods

1.2.1 Apparatus and Chemicals

1.2.1.1 Apparatus

- Analytical balance (Mettler Toledo (AL204), Maximum capacity 21 g with ± 0.01 g)
- Vacuum filtration setup
- Water bath (Fischer Scientific GDP 05, with ambient to 95 °C temperature range, ± 0.02 °C temperature uniformity, with 5L bath volume)
- Autoclave, (HV-85, Artisan Technology group)
- Ice bath
- Pyrex Desiccator
- HPLC system with Bio-Rad Aminex HPX-87 H column and Shimadzu reactive index column
- HPAEC system with Dionex GP50 pump, ED40 Detector, AS50 Autosampler
- Digital oil bath (Thermohaake DC-30, -50 °C to 200 °C temperature range with ± 0.01 K accuracy)
- Gravity convention drying oven (Fischer brand Isotemp general purpose heating and drying oven with 65 L capacity and temperature range from 50 °C to 250 °C with ± 4 °C uniformity)
- Muffle furnace
- General purpose Parr vessel with maximum temperature and pressure 300 °C and 115 bar accordingly (Alloy 20 carpenter 20, 22 mL with Fe- 35 %, Ni- 34%, Cr -20%, Mo-2.5%, Mn- 0.7%) wrench (21AC4), Bench socket (A22AC3)

- Swagelok 314 Stainless steel double ended cylinders (DOT -3A 1800 WITH 1800 psig pressure rating)
- Fischer AccuSpin 400 Centrifuge (400 mL capacity, 30 to 13000 rpm speed range,

1.2.1.2 Reagents

- 72 % H₂SO₄ (Ricca Chemical Company (71.8-72.2% w/w), Specific gravity 1.6338 at 20 °C)
- High purity standards D (+) glucose, D (+) xylose, D (+) mannose, D (+) galactose, levulinic acid (Purchased from Sigma Aldrich with 98 % purity, density 1.134 g/mL), formic acid (Purchased from Sigma Aldrich with 95- 97% purity, density 1.22 g/mL at 25 °C), acetic acid (purchased from Fischer scientific with 99.7% w/w, density 1.05 g/mL at 25 °C), D- mannitol (98+%, purchased from Acros Organics), glucuronic acid, sugar kelp (*Saccharina latissima*)
- Deionized water
- Heat transfer fluid (Clearco Products Co. Inc. DPOM-400 Silicone bath fluid, temperature range for open system 25 °C to 250 °C, specific gravity 1.07)
- HPLC grade Millipore water
- Pure Chemicals for sugar analysis of individual carbohydrates such as laminarin (Purchased from.....), Sodium Slat of Alginic Acid (Purchased from...), Fucoidan (Purchased from....), Carrageenan (Purchased from....) and cellulose (Purchased from...)

1.2.1.3 Materials

- Glass beakers (Fischer brand 100mL, 250 mL, 300 mL and 600 mL capacity)
- Test tubes (18x150 mm, #2048-00150)
- Teflon stir rods that fits in test tube with around 5 cm longer than test tube

- Pyrex Filter flasks with 1000 mL capacity and filtering crucibles
- Adjustable pipette with range from 0.02 mL to 5 mL
- Dow corning high vacuum grease to smooth the surface of Parr reactor tank and to decrease the friction
- Autoclave wide mouth approximate 500 mL volume capacity bottles with Ezvialz seals
- Disposable latex free Syringes with 10 mL capacity and Cell treat Scientific syringe filter with 0.45 μm x13 mm diameter # 229754
- Auto sampler HPLC vials (Fischer brand 10-425 screw thread # 03-391-16) with PTFE closure
- Auto sampler HPAEC vials

1.2.2 Sample Preparation

Sugar kelp (*Saccharina latissima*) was harvested during June in Saco Bay, ME, USA and were kindly provided by Adam St. Gelais and Carrie Byron at the University of New England. The sugar kelp was washed under running water to remove salts and other contaminants from the surface of the sugar kelp leaves. The sugar kelp samples were dried using freeze dryer at -20, -10, 0, 10, and 25 °C for 4 h at each temperature. After drying, the sugar kelp samples were grounded into a fine powder using a Wiley mill into < 0.5 mm particle size and these powder samples were sieved to get uniform particle size. These powdered samples were stored in the refrigerator to avoid any light interference for compositional analysis.

1.2.3 Physiochemical Analysis

1.2.3.1 Moisture Content

The moisture content of freeze dried sugar kelp was calculated by ASTM E1756-01 procedure. Initially, crucibles were identified by using porcelain marker and dried in a conventional oven at

105 ± 5 °C for 4 h until a constant weight was achieved. Around 500 ± 0.02 mg of the sugar kelp powder was weighed in oven dried crucible and was put into conventional oven at 105 ± 5 °C. After 24 h, the hot crucibles were cooled to room temperature in the desiccator for an hour. The moisture content of the sugar kelp was expressed in dry basis as a gram of water per 100 g of dry solids (42).

1.2.3.2 Ash Content:

The presence of inorganic materials was determined according to NREL/TP-5100-60943 “Summative Mass Analysis of Algal Biomass- Integration of Analytical Procedure”. A 3 ± 0.05 g sample of pre-grounded freeze-dried dry sugar kelp powder was weighed in oven dried crucible. A porcelain marker identified crucible was placed in the muffle furnace at 575 ± 5°C. After 12 h, the hot crucible was transferred into the desiccator to cool it down to the room temperature. The final weight of the crucible with sample was weighed. The crucible was dried in conventional oven until constant weight was achieved. Then dried crucible was placed in muffle furnace at 575 ± 5 °C with seaweed powder for 24 h until constant weight was achieved. The ash content of algae biomass was calculated by:

$$\% \text{ Ash} = \frac{(\textit{Weight of crucible + ash}) - \textit{weight of oven dried crucible + ash}}{\textit{Oven dried weight of algae biomass}} * 100$$

Equation 1 % Ash

1.2.3.3 Protein Content:

The total nitrogen content was determined by an elemental analyzer. This analyzer provides the fraction of carbon, hydrogen and nitrogen in sugar kelp powder. The protein content of the algae biomass can be estimated from the nitrogen content, by using a nitrogen to protein conversion multiplier. The conversion multiplier, also known as Jones factor 5.4 (for sugar kelp), is based on the existence of all nitrogen in sugar kelp as protein (43). The equation for protein measurement is:

$$\% \text{ of Protein} = \% \text{ of Nitrogen content} \times 5.4 \text{ (Nfactor)}$$

Equation 2 % of Protein

1.2.3.4 Lipid Content and carbohydrate content:

The lipid content was determined by AOAC method using the acid hydrolysis- hydrochloric acid in methanol (Sappati et al). It was found that the average fat/lipid content in sugar kelp was in the range of 2 to 4% based on acid hydrolysis of different sugar kelp (44). Carbohydrate content was determined by the difference method based on all other proximate content. It is expressed as grams of carbohydrate per 100 g of total dry solid.

1.2.4 Sugar Analysis of Sugar Kelp

Glucose content of brown sugar kelp was determined using the acid hydrolysis procedure (46). This acid hydrolysis was done in two stages and tested at different temperature, reaction time and acid concentrations. Approximately, 100 ± 5 mg of sugar kelp powder and 1 ± 0.1 mL of 72% H_2SO_4 are mixed in a test tube using a stir rod. The sample was mixed until the sugar kelp powder particles were fully in contact with sulfuric acid. Then the test tubes were placed in water bath at 40 ± 3 °C for 60 min. The solution was stirred every 5 ± 1 minute using Teflon rod without taking test tube out of water bath. After completion of hydrolysis reaction, test tubes were transferred in

to the ice bath for 5 min retention time to stop the reaction. The sample was diluted using a specific amount of deionized water and the diluted solution was transferred into autoclave bottles, sealed, kept on the autoclave safe rack. The reaction condition of the autoclave was 121 °C for specific residence times of 1h, 2.5h, and 4h. After the completion of reaction, the autoclave was cooled down to 75 °C and the samples were taken out. The bottles were transferred into ice bath for 5±1 min to stop the reaction. Then the sample was taken out by removing the cap of autoclave bottles. The sample was filtered and transferred into an HPLC vial for sugar analysis of hydrolyzed sample.

1.2.5 Acid Hydrolysis of Sugar Kelp at High Temperature

In two stage acid hydrolysis of sugar kelp, the first stage is the same as glucose analysis experiment at low temperature and high acid concentration. After digesting the sugar kelp powder in concentrated acid it was diluted to the desired acid concentration for the next hydrolysis step and filtered. Filtration was done by weighing the diluted solution and vacuum filtering the sample. The filtered liquid was transferred into a pre-weighted clean glass beaker and the weighed sample and beaker were sealed with paraffin film and kept in a refrigerator at 4 °C until further hydrolysis at high temperature. The filtered solid particles on the filter paper were transferred into a clean beaker and dried at 105 °C for 12 h. The beaker then was cooled down in desiccator to room temperature and the weight of the beaker with dried solids and filter paper was taken. The weight difference before and after filtration was compared. The filtered liquid was used for high temperature hydrolysis. A general purpose Parr vessel (reactor) was washed and dried very well and the weight of the vessel was measured with and without filtered liquid. The next step was to evaluate the condition of the reactor gasket for safety purpose. A special wrench was used to firmly secure the reactor screw cap using the bench socket. It was necessary to check the screw cap to prevent any kind of leakage or accident while heating. After this, the reactor was set in an oil bath supported

by a stand to ensure that the tank was fully immersed in the oil bath at the predetermined temperature setting of oil bath. At reaction completion, the reactor was transferred to a water bath at 25 ± 5 °C for 3 min to decrease the reactor temperature slowly. Then the reactor was transferred into an ice bath for 2 min and the reactor was dried with clean rag and paper towel to remove the oil and water drops. Then the reactor was opened with a wrench and weighed again to measure the weight difference of reactor with sample before and after the hydrolysis and the weight of the sample and empty tank. The sample was filtered and was transferred into HPLC vials for HPLC analysis.

1.2.6 Three Stage Hydrolysis of Sugar Kelp

Three stage hydrolysis is a combination reaction process consisting of the 2-step glucose analysis of sugar kelp followed by the high temperature acid hydrolysis to generate levulinic acid. In this process, the first step and second step were the same as previously explained in glucose analysis of sugar kelp. After the second step, the hydrolyzed liquid was filtered in the vacuum filter and it was followed by the same procedure as was explained in acid hydrolysis of sugar kelp at a high temperature after the vacuum filtration step.

1.2.7 Acid Hydrolysis of Pure Individual Carbohydrates

Acid hydrolysis of individual carbohydrates was performed to identify the chemical decomposition of each carbohydrate into sugar monomers by sugar analysis and high temperature acid hydrolysis. The chemical composition of brown seaweed varies with cultivation, harvesting time, weather and geographic location (44,47,53). Moreover, highly dominated hydrocarbons in brown seaweed are Laminarin, Mannitol, Alginate, Fucoidan and Carrageenan. Most of these carbohydrates are reported to be good nutritional sources for food products. However, the presence of C6 sugar

chains can be also useful to convert them into glucose and other sugar monomers and eventually into Levulinic Acid.

The sugar analysis of pure polysaccharides was carried in a sealed pressure tube by repeating the same method as explained earlier in sugar analysis of sugar kelp with concentrated acid (72 wt%) for 60 min retention time followed by diluted acid (4 wt%) at 121 °C for residence time of 60 min and 240 min. The sample was taken out from autoclave bottles by removing the seal caps and filtered and transferred into HPLC vials for HPLC analysis

High temperature acid hydrolysis of pure polysaccharides was performed by following the same procedure as explained earlier for acid hydrolysis of sugar kelp with concentrated acid (72 wt%, 40 °C) at low temperature following by diluted acid (4 wt%) at high temperature in a general purpose Parr vessel at 175 °C with 80 min retention time. At the completion of reaction, the reactor was transferred into an ice bath and cooled down to room temperature, after which the sample was filtered and transferred into an HPLC vial for HPLC analysis.

1.2.8 Analytical Methods

A stock solution containing all monosugars and acids was precisely prepared at the following target concentrations for HPLC analysis:

- D (+) Glucose (0.5 g per 1000 mL)
- D (+) Xylose (0.1 g per 1000 mL)
- D (+) Mannose (0.1 g per 1000 mL)
- D (+) Galactose (0.1 g per 1000 mL)
- D (-) Arabinose (0.5 g per 1000 mL)
- D Mannitol (0.5 g per 1000 mL)
- Glucuronic acid (0.5 g per 1000 mL)

- Formic acid (0.5 g per 1000 mL)
- Acetic acid (0.5 g per 1000 mL)
- Levulinic acid (0.5 g per 1000 mL)

To prepare the standard solutions, a stock solution was diluted in 5 different vials (C1 – C5) with exact amounts of: C1 (2 mL of stock solution+ 8 mL of deionized water), C2 (4 mL of stock solution +6 mL of de-ionized water), C3 (6 mL of stock solution + 4 mL de-ionized water), C4 (8 mL of stock solution + 2 mL de-ionized water) and C5 (10 mL of stock solution). Solutions were mixed well and transferred to HPLC vials.

The composition of the hydrolyzed liquid mixture was determined by HPLC analysis. All samples were filtered with a syringe filter to prevent clogging of solids in HPLC column. The HPLC system (Shimadzu) was equipped with a Bio-Rad Aminex HPX-87H column (CTO-10 A), SIL-20 AC auto sampler, a Shimadzu refractive index detector, and LC-10 AT pump. The mobile phase consisting of an aqueous solution of sulfuric acid (5 mM) with 0.6 mL/min flowrate and column was operated at oven temperature of 45 °C. The analysis of the sample was done with retention time of 65 min and 120 min. The concentration of each compound was determined using a calibration curve of standard solutions with known concentrations. Consequently, High Performance Anion Exchange Chromatography with Pulsed Amperometric Detection (HPAEC-PAD) was used to analyze mono sugars of acid hydrolyzed solution. The column of this instrument consisted of Dionex CarboPac PAI (4×250 mm) with oven temperature of 30°C, Dionex Carbopac PAI (4 × 50 mm) guard column, Dionex IonPac NGI (4 × 35 mm) guard column, with GP50 pump, ED40 gold detector, AS50 auto sampler. The total flow rate of eluent was 1 mL/min (eluent A as degassed water at 0.7 mL/min and eluent C as 300 mM NaOH from post column with flowrate of 0.3 mL/min).

1.2.9 Statistical Analysis

Statistical analysis of each experiments was performed in triplicate. The results of analysis are performed in mean \pm standard deviation. Multiway ANOVA (Analysis of Variance) was performed to evaluate the effect ($p \leq 0.05$) of each independent variable such as time, temperature and acid concentration on each level and interaction effect on the yield of levulinic acid. Tukey's honest significant difference post hoc test was performed to identify any significant differences between the means of comparable treatment.

1.3 Results and Discussion

Table 2 Physiochemical results of Seaweed on dry basis

Moisture Content (g/100 g of freeze dried solids)	Ash Content (g/100 g of freeze dried solids)	Protein Content (g/100 g of freeze dried solids)	Lipid Content (g/100 g of freeze dried solids)	Carbohydrate Content (g/100 g of freeze dried solids)
6.01 \pm 0.1%	33 \pm 0.3%	10.41 \pm 0.1%	2.08 \pm 0.1%	48.5 \pm 0.1%

1.3.1 Moisture Content

The moisture content of biomass is highly varied at different weather conditions. The major components affecting the moisture content of seaweed are the structural difference of the tissue, size, weather condition and growing environment (48). Sappati et al., showed that the moisture content of seaweed samples decreases as the temperature increases due to weather or harvesting period (44).

1.3.2 Ash Content

The presence of structural (inorganic material that is attached in the physical structure of the seaweed) or extractable inorganic materials (that can be removed by washing) are considered as

the total ash composition. Research shows that the mineral content (mainly K, Na, Ca, Mg, I) of macro algae is higher than terrestrial plants, which are around 20% more than grains (47). High mineral content of seaweed is a good source of minerals for human food. But this inorganic material of seaweed limits the conversion of seaweed in biofuels because of its high capacity to reduce the acidity of acids.

1.3.3 Fat Content

The fat content of brown seaweed is usually in the form of saturated fatty acids, palmitic acid, stearic acid and polyunsaturated acid (44). The fat content of brown seaweed depends upon physiochemical state, life cycle, seasonal and environmental factors, nutrition availability and sun light (49).

1.3.4 Protein Content

Likewise, other chemical constituents, the protein content also varies with seasonal variation, geographic location, environmental condition and growth (44). The protein content is usually calculated by considering the Jones factor which is the ratio of protein to nitrogen as 6.25 (50). However, other research considered the factor as 5.38 for brown seaweed due to presence of non-protein nitrogen content (51). The average nitrogen content is not affected by the seasonal variation of seaweed. In *Saccharina latissima*, the average nitrogen content was noted as 1.93 ± 0.01 g per 100g of freeze dried basis. The values of protein content are quite identical with the results from Sciender's sugar kelp analysis which is around 10.65 ± 0.53 g per 100 g of freeze dried basis (53).

1.3.5 Carbohydrate Content

Results shown in Table 2 present carbohydrate composition calculated as the mass difference remaining after other fractions are accounted for. This is in part because the variety of different

carbohydrates and polysaccharides found in seaweeds. The polysaccharide of seaweed varies based on species and environmental conditions. Brown seaweed has been known for its rich carbohydrate content. The carbohydrate exists on the primary cell wall of seaweed in two forms: structural and storage. Structural function of macroalgae protects seaweed from dehydration, waves and some severe ocean conditions (52). Cellulose and alginate are an example of structural components, whereas, laminarin, fucoidan and mannitol are examples of storage carbohydrates. Alginate is a structural linear polysaccharide composed of β -D- mannuronic acid (M) and α -L- guluronic acid (47). Guluronic acid has a mechanism of gelation which determines gel strength. Figure 6 shows the structure of alginate (54).

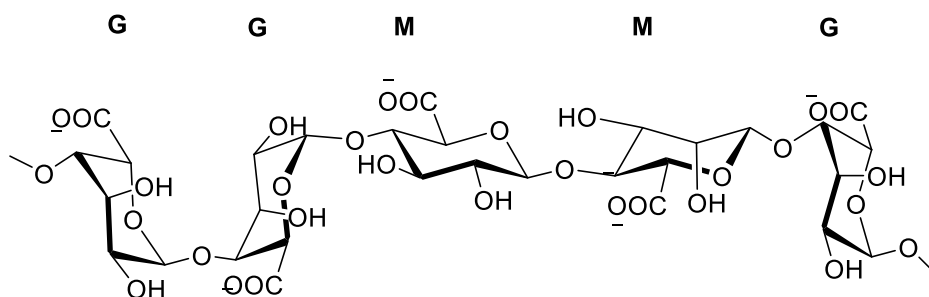


Figure 6 Alginate Structure

D-Mannitol is a six-carbon sugar alcohol in brown algae. The content of mannitol in seaweed depends upon the harvesting condition and type of seaweed which could be dominated around 20-30% by dry weight in brown seaweed (55). The extraction of mannitol in seaweed can be used as carbon source for ethanol production. Scheiner at al., found the highest yield of mannitol in autumn period which is round 24-27 % by dry weight of brown seaweed (55). Figure 7 shows the chemical structure of Mannitol.

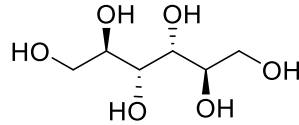


Figure 7 Chemical structure of Mannitol

Cellulose is a linear structural polysaccharide in brown seaweed. It is an important component of primary cell wall in seaweed and it linked as β (1-4) D-glucose residue. Schinder et al., found that the composition of cellulose also depends upon the seasonal variation and type of seaweed. However, the domination of cellulose in sugar kelp is up to 8% of dry weight (56). The crystalline structure of cellulose exists in two form: α -cellulose and β -cellulose (47).

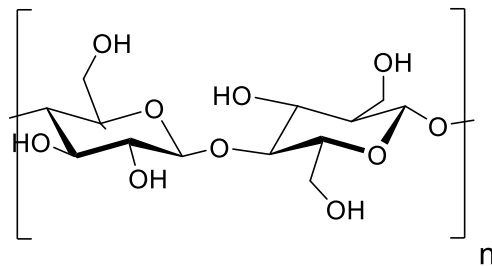


Figure 8 Linear Structure of cellulose

Laminarin is storage carbohydrate in the plastids of each cell in brown seaweed (47). Laminarin is used as a carbon source for algae during winter. It is a linear polysaccharide consisting of glucose monosaccharides units linked with β -(1,3) D-glucose bond or β -1,6 glycosyl bonds and β -(1,2)-D-glycosyl units (57). The presence of M-chain and G-chain proves the existence of D-Mannitol and D-glucose respectively (57). The solubility of laminarin in cold water or hot water depends upon the number of branches. Linear branches are more soluble in cold water (57). Scheiner et al., report that the highest level of laminarin in brown seaweed occurs during the summer or autumn and the lowest level occurs in winter (53).

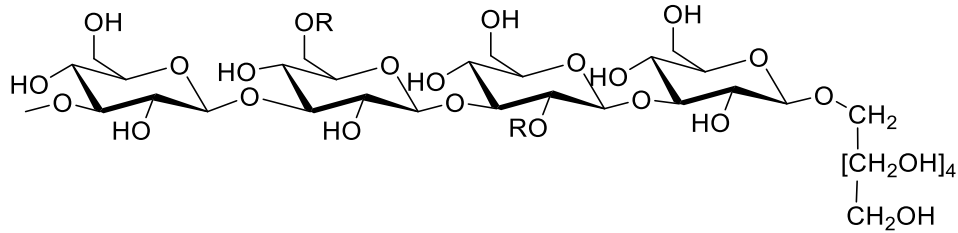


Figure 9 Possible Laminarin Structure with D-Mannitol (M-chain) Residues at the end (58)

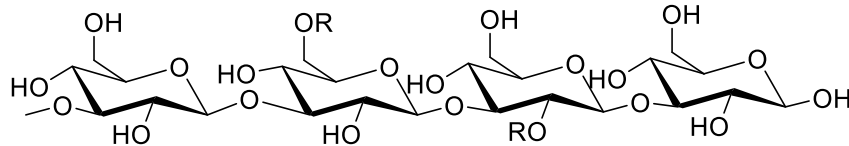


Figure 10 Possible Laminarin Structure with D-glucose (G-chain) Residues at the end (58)

1.3.6 Sugar Analysis of Seaweed

The purpose of pretreatment and scarification is to decompose the complex cell walls of *Saccharina latissima* into polymers and molecules, which could be further converted into chemicals and biofuels. The major chemical composition of *Saccharina latissima* is cellulose, laminarin, alginate, mannitol and fucoidan. Pretreatment with concentrated acid breaks down the rigid and insoluble cellulose into an amorphous water soluble solution. Moreover, it also breaks down the intermolecular bonds of *laminaria saccharina* and converts them into simple monomers which increases the accessibility for further reaction. After pretreatment with concentrated acid, sugar analysis experiments of *Laminaria saccharina* were performed with diluted sulfuric acid in a concentration range of 2%,4%,6%,8% and 10% wt% at three different residence times to determine the yield of glucose at 121 °C. The results in Table 3 Table 2 Physiochemical results of Seaweed on dry basis show that the glucose yield was increased at low acid concentration with high retention time but at 6 wt % H₂SO₄ the glucose yield doesn't show any yield difference between 150 min and 240 min. However, the glucose yield was decreasing at higher concentration with high retention time. In addition to this, for lower acid concentration, the glucose yield shows the function of acid concentration and retention time. The optimum yield of glucose reaches 8 wt%

with 150 min retention time. So, there could be a breaking down of laminarin structure at high acid concentration and high retention time, because intermolecular bonds of laminarin have higher activation energy compared to cellulose structure. In addition, the high acid concentration also creates problems such as corrosion of the reactor, so there is a need of expensive reactor materials and separation and regeneration of catalyst becomes very complicated. However, for diluted acid, ammonia can neutralize the acid and further solution of ammonium sulfate could be used as a fertilizer.

1.3.7 AHDH of Sugar Kelp at High Temperature (two stage acid hydrolysis)

Levulinic acid is derivation from cellulose and hexose monomers are illustrated by the mechanisms shown in Figure 11 and Figure 12. An objective of this process was to optimize yield of levulinic acid by varying three different variables of temperature (in the range of 150°C and 200°C), time (in the range of 40 min and 120 min) and acid concentration (in the range of 4 wt% and 8 wt%). Statistical analysis (Multiway analysis of variance) shows the effect of different variables on the yield of levulinic acid. The results show that at low acid concentration, the yield of levulinic acid is a function of temperature and time. Statistical analysis reveals that at temperatures from 150 °C to 175 °C, the yield of levulinic acid becomes the function of temperature, however, in the temperature range of 175 °C to 200 °C temperature no longer makes a big difference in the yield of levulinic acid, so 175 °C is the optimum for the yield of levulinic acid (Table 3). Looking at time, 80 min is the best retention time for the conversion of hexose sugars into levulinic acid. At lower retention time, the conversion is less and at high retention time, side reactions of cellulose decrease the conversion of cellulose into levulinic acid.

There is no generally accepted pathway for the conversion of laminarin to levulinic acid. The hydrolysis of pure laminarin shows that the intermolecular bond requires severe conditions

compared to cellulose to break down the intermolecular bond of glucan. We believe that higher temperature and acid concentration breaks down more β (1-4) linkage of cellulose than β (1-3) and β (1-6) linkage of laminarin. However, low domination of hexose content in seaweed decreases the yield of seaweed based on mass%. The highest yield we obtained was $4.12 \pm 0.05\%$ at 200°C with 40 min retention time with 6 wt% H_2SO_4 , though it was noted that acid concentration has very low effect on the yield of levulinic acid.

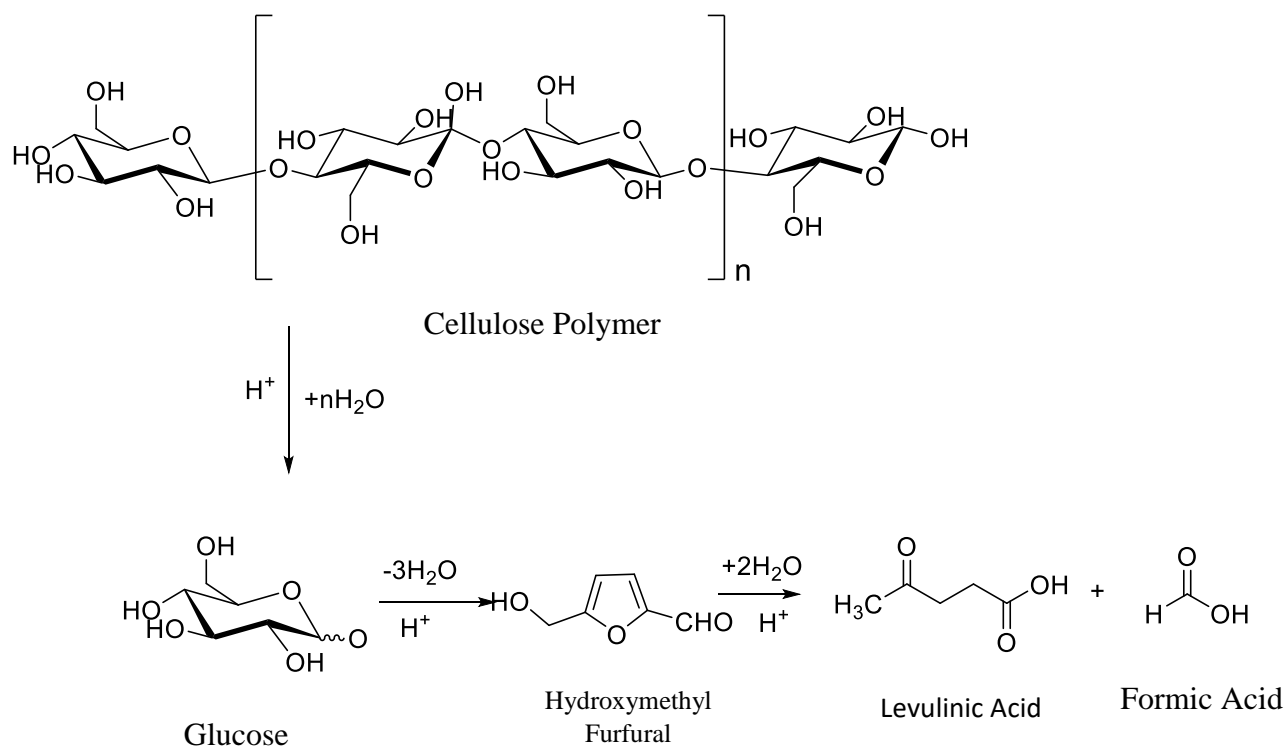


Figure 11 Acid catalyzed pathway of cellulose to Levulinic acid

1.3.8 Three Stage Hydrolysis and Dehydration of Sugar Kelp

The purpose of three stage acid hydrolysis was to line up the glucose content of seaweed at high temperature and different retention time. The reason behind this study is to calculate the conversion of glucose into levulinic acid. However, results of glucose from sugar analysis were the strong

function of acid concentration. Multiway ANOVA shows the impact of temperature and retention time has a high impact on levulinic acid yield whereas, acid concentration has little effect. However, comparison between Table 5 and Table 7 shows that the yield of levulinic acid decreases in three stage hydrolysis compared to direct conversion of cellulose and laminarin. One reason to explain these data could be that glucose is degraded from repeated exposure to elevated temperature and is converted into humin by side reaction which decreases the conversion into levulinic acid (60). Moreover, at the most severe conditions, we noticed also a color change of hydrolyzed samples from light brown to green along with a change of color on the surface of the reactor.

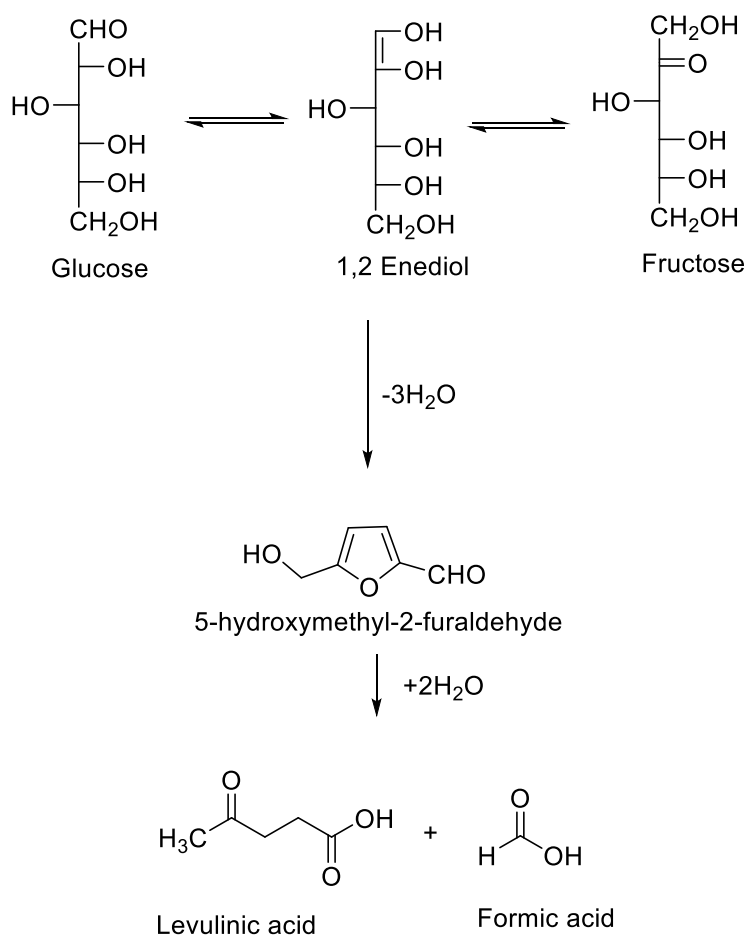


Figure 12 Acid hydrolysis pathway from conversion of glucose to levulinic acid

Table 3 Sugar Analysis Results of Sugar Kelp

	2% H₂SO₄	4% H₂SO₄	6% H₂SO₄	8% H₂SO₄	10% H₂SO₄
60 min	17.23±0.75%	19.38±0.56%	21.10±0.58%	25.82±0.87%	20.51±3.27%
150 min	19.32±0.67%	21.41±0.23%	24.94±2.21%	28.66±1.04%	23.66±0.50%
240 min	22.07±0.96%	25.74±0.27%	25.00±1.40%	23.58±0.50 %	21.68±0.55%

(presented as mol%, by assuming total glucan content 19%, at 121 ° C)

Table 4 Levulinic Acid as a Byproduct from Sugar Analysis of Sugar Kelp

	2% H₂SO₄	4% H₂SO₄	6% H₂SO₄	8% H₂SO₄	10% H₂SO₄
60 min	N.D.	N.D.	N.D.	2.55±0.12%	2.28±0.34%
150 min	N.D.	N.D.	2.50±0.20%	6.39±0.31%	5.94±0.14%
240 min	N.D.	0.60±0.73%	3.07±0.29%	6.58±0.26%	8.89±0.47%

(based on mol%, assuming total glucan content 19%)

N.D.: Not Detected

Table 5 Levulinic Acid Results from Two Stage Acid Hydrolysis (based on mol%)

	4% H ₂ SO ₄			6% H ₂ SO ₄			8% H ₂ SO ₄		
	150 °C	175 °C	200°C	150 °C	175 °C	200°C	150 °C	175 °C	200°C
40 min	5.62±0.70 % bBx	20.64±0.83 % aBx	28.24±1.07 % aBx	10.50±3.24 % bAx	27.66 ±0.63% aAx	30.44±0.37 % aAx	16.21±0.12 % bAx	27.60±0.26 % aAx	26.55±3.41 % aAx
80 min	15.01±1.15 % bBxy	28.13±0.83 % aBxy	29.65±1.69 % aBxy	18.39±0.16 % bAxy	28.51±0.44 % aAxy	30.09±0.88 % aAxy	24.03±0.05 % bAxy	28.44±0.11 % aAxy	25.67±0.81 % aAxy
120 min	19.00±0.19 % bBy	29.30±0.04 % aBy	30.11±0.06 % aBy	20.83±0.04 % bAy	28.39±0.17 % aAy	25.03±0.33 % aAy	26.73±0.08 % bAy	29.15±0.03 % aAy	22.76±0.21 % aAy

Results are mean ± standard deviation of triplicate for each sample (n = 3). Significant differences between the values are measured at p < 0.05. Small letters (a, b) denote row-wise comparison between treatments or with temperatures. Capital letters (A, B) denote comparison between acid concentration. Small letters (x,y) denote comparison between time.

Table 6 Levulinic Acid Results from Two Stage Acid Hydrolysis (based on mass%)

	4% H ₂ SO ₄			6% H ₂ SO ₄			8% H ₂ SO ₄		
	150 °C	175 °C	200°C	150 °C	175 °C	200°C	150 °C	175 °C	200°C
40 min	0.49±0.43% bBx	2.79±0.11% aBx	3.82±0.14% aBx	1.42±0.44% bAx	3.74±0.09% aAx	4.12±0.05% aAx	2.19±0.02% bAx	3.74±0.04% aAx	3.59±0.46% aAx
80 min	2.03±0.16% bBxy	3.81±0.21% aBxy	4.01±0.23% aBxy	2.49±0.02% bAxy	3.86±0.06% aAxy	4.07±0.12% aAxy	3.25±0.01% bAxy	3.85±0.01% aAxy	3.47±0.11% aAxy
120 min	2.57±0.03% bBy	3.97±0.01% aBy	4.07±0.01% aBy	2.82±0.00% bAy	3.84±0.02% aAy	2.70±0.04% aAy	3.62±0.01% bAy	3.95±0.00% aAy	3.08±0.03% aAy

Results are mean ± standard deviation of triplicate for each sample (n = 3). Significant differences between the values are measured at p < 0.05. Small letters (a, b) denote row-wise comparison between treatments or with temperatures. Capital letters (A, B) denote comparison between acid concentration. Small letters (x,y) denote comparison between time.

Table 7 Levulinic Acid Results for Three Stage Acid Hydrolysis (based on mol%)

	4% H ₂ SO ₄			6% H ₂ SO ₄			8% H ₂ SO ₄		
	150 °C	175 °C	200°C	150 °C	175 °C	200°C	150 °C	175 °C	200°C
40 min	5.79±0.40 % bBx	21.89±1.73 % aBx	24.89±1.21 % aBx	6.89±0.38 % bAx	18.07±1.48 % aAx	21.68±3.13 % aAx	10.76±0.77 % bAx	21.89±1.73 % aAx	18.56±1.02 %aAx
80 min	12.81±0.67 % bBy	24.24±1.26 % aBy	27.01±0.42 % aBy	14.40±1.37 %bAy	18.78±1.81 % aAy	19.77±1.30 % aAy	12.02±0.28 %bAy	21.15±4.32 %aAy	18.24±0.92 % aAy
120 min	18.67±2.6 % bBy	24.35±3.12 % aBy	25.17±0.80 % aBy	15.90±1.42 % bAy	23.01±3.84 % aAy	19.10±0.76 % aAy	15.19±2.36 % bAy	18.23±1.10 % aAy	16.88±0.64 % aAy

Results are mean ± standard deviation of triplicate for each sample (n = 3). Significant differences between the values are measured at p < 0.05. Small letters (a, b) denote row-wise comparison between treatments or with temperatures. Capital letters (A, B) denote comparison between acid concentration. Small letters (x,y) denote comparison between time

Table 8 Levulinic Acid Results for Three Stage Acid Hydrolysis (base on mass%)

	4% H ₂ SO ₄			6% H ₂ SO ₄			8% H ₂ SO ₄		
	150 °C	175 °C	200°C	150 °C	175 °C	200°C	150 °C	175 °C	200°C
40 min	0.78±0.05% bBx	2.37±0.58% aBx	3.37±0.16% aBx	0.93±0.05% bAx	2.45±0.20% aAx	2.93±0.42% aAx	1.46±0.10% bAx	2.96±0.23% aAx	2.51±0.14% aAx
80 min	1.95±0.19% bBy	3.28±0.17% aBy	3.66±0.06% aBy	2.06±0.32% bAy	2.54±0.25% aAy	2.86±0.18% aAy	2.15±0.19% bAy	2.86±0.58% aAy	2.47±0.13% aAy
120 min	2.53±0.36% bBy	3.30±0.42% aBy	3.41±0.11% aBy	1.63±0.04% bAy	3.11±0.52% aAy	2.58±0.10% aAy	1.73±0.09% bAy	2.47±0.15% aAy	2.28±0.09% aAy

Results are mean ± standard deviation of triplicate for each sample (n = 3). Significant differences between the values are measured at p < 0.05. Small letters (a, b) denote row-wise comparison between treatments or with temperatures. Capital letters (A, B) denote comparison between acid concentration. Small letters (x,y) denote comparison between time.

Table 9 Levulinic Acid Results from Two Stage Acid Hydrolysis (based on Carbohydrate 48.5%)

	4% H ₂ SO ₄			6% H ₂ SO ₄			8% H ₂ SO ₄		
	150 °C	175 °C	200°C	150 °C	175 °C	200°C	150 °C	175 °C	200°C
40 min	1.37±1.21 % bBx	7.89±0.32 % aBx	10.80±0.41 % aBx	4.01±1.24 % bAx	10.58 ±0.24% aAx	11.64±0.14 % aAx	6.20±0.05 % bAx	10.55±0.10 % aAx	10.15±1.30 % aAx
80 min	5.74±0.44 % bBxy	10.76±0.61 % aBxy	11.34±0.64 % aBxy	7.03±0.06 % bAxy	10.90±0.17 % aAxy	11.50±0.34 % aAxy	9.19±0.02 % bAxy	10.88±0.04 % aAxy	9.81±0.31 % aAxy
120 min	5.70±2.70 % bBy	11.20±0.01 % aBy	11.51±0.02 % aBy	7.97±0.01 % bAy	10.86±0.06 % aAy	7.64±0.12 % aAy	10.22±0.03 % bAy	11.15±0.01 % aAy	8.70±0.08 % aAy

Results are mean ± standard deviation of triplicate for each sample (n = 3). Significant differences between the values are measured at p < 0.05. Small letters (a, b) denote row-wise comparison between treatments or with temperatures. Capital letters (A, B) denote comparison between acid concentration. Small letters (x,y) denote comparison between time.

Table 10 Levulinic Acid Results for Three Stage Acid Hydrolysis (based on carbohydrate percentage)

	4% H ₂ SO ₄			6% H ₂ SO ₄			8% H ₂ SO ₄		
	150 °C	175 °C	200°C	150 °C	175 °C	200°C	150 °C	175 °C	200°C
40 min	2.22±0.15 % bBx	6.70±1.65 % aBx	9.52±0.46% aBx	2.63±0.14 % bAx	6.91±0.57 % aAx	8.29±1.20 % aAx	4.12±0.30 % bAx	8.37±0.66 % aAx	7.10±0.39 % aAx
80 min	4.90±0.26 % bBy	9.27±0.48 % aBy	10.33±0.16 % aBy	5.51±0.52 % bAy	7.18±0.69 % aAy	7.56±0.50 % aAy	4.60±0.11 % bAy	8.09±1.65 % aAy	6.97±0.35 % aAy
120 min	7.14±1.03 % bBy	9.31±1.19 % aBy	9.62±0.30% aBy	6.08±0.54 % bAy	8.80±1.47 % aAy	7.30±0.29 % aAy	5.81±0.90 % bAy	6.97±0.42 % aAy	6.45±0.25 % aAy

Results are mean ± standard deviation of triplicate for each sample (n = 3). Significant differences between the values are measured at p < 0.05. Small letters (a, b) denote row-wise comparison between treatments or with temperatures. Capital letters (A, B) denote comparison between acid concentration. Small letters (x,y) denote comparison between time.

Table 11 Acid Hydrolysis of Individual Carbohydrates

Used Carbohydrate for analysis	Inlet wt (mg)		Mass of Analyze		
			Sugar/ intermediate concentration (mg)		Mass of final analyze (171 °C, 80 min)
			240 min	60 min	
Laminarin (from Thelus laminarie)	100±05	Levulinic Acid	2.27±0.24	0.49±0.09	34.55±1.63
		Formic Acid	2.32±0.26	1.40±0.52	17.00±0.81
		Glucose	40.52±7.85	48.08±6.48	18.91±23.51
		Arabinose	0.52±0.57	N.D.	0.57±0.01
		XMG	0.26±0.03	0.11±0.01	1.53±0.10
		Mannitol	0.15±0.01	N.D.	N.D.
		Glucuronic Acid	0.09±0.06	0.07±0.05	N.D.
Mannitol	100±05	Levulinic Acid	N.D.	N.D.	0.45±0.01
		Formic Acid	N.D.	N.D.	N.D.
		Glucose	0.11±0.16	N.D.	0.33±0.23
		Arabinose	N.D.	N.D.	48.39±0.36
		XMG	N.D.	N.D.	N.D.
		Mannitol	312±16.43	406.59±14.37	48.74±0.40
		Glucuronic Acid	N.D.	N.D.	N.D.
Alginate	100±05	Levulinic Acid	N.D.	N.D.	2.25±0.11
		Formic Acid	0.92±0.02	3.02±0.15	2.20±0.09
		Glucose	2.15±0.04	7.42±0.32	2.29±0.24
		Arabinose	0.38±0.00	0.43±0.02	0.48±0.01
		XMG	0.53±0.01	0.15±0.09	3.69±0.14
		Mannitol	N.D.	N.D.	N.D.
		Glucuronic Acid	N.D.	N.D.	0.09±0.00

Table 11 Continued

Fucoidan	50.8±05	Levulinic Acid	0.09 ±0.12	N.D.	2.67±0.12
		Formic Acid	0.76±0.09	N.D.	5.13±0.17
		Glucose	N.D.	N.D.	0.26±0.03
		Arabinose	N.D.	N.D.	N.D.
		XMG	0.86±0.09	1.04±0.07	0.35±0.02
		Mannitol	0.15±0.02	N.D.	N.D.
		Glucuronic Acid	0.20±0.15	0.25±0.02	N.D.
Carrageenan	100±05	Levulinic Acid	13.20±1.48	10.65±0.24	28.11±0.25
		Formic Acid	5.96±0.66	5.58±0.12	12.93±0.33
		Glucose	0.04±0.01	N.D	0.82±0.02
		Arabinose	0.86±0.08	1.05±0.02	0.86±0.01
		XMG	8.97±0.99	12.16±0.24	0.19±0.00
		Mannitol	N.D	N.D	N.D
		Glucuronic Acid	N.D	N.D	0.15±0.21
Glucuronic Acid	100±05	Levulinic Acid	N.D	N.D	2.27±0.25
		Formic Acid	0.57±0.42	1.59±0.17	1.45±0.16
		Glucose	0.99±0.12	0.21±0.02	1.93±0.22
		Arabinose	0.09±0.01	0.08±0.01	0.43±0.01
		XMG	0.80±0.10	0.68±0.08	3.81±0.29
		Mannitol	N.D	N.D	N.D
		Glucuronic Acid	29.50±4.52	57.81±3.58	0.13±0.02

1.4 Conclusion

This study performed acid catalyzed hydrolysis of sugar kelp in to levulinic acid using two different routes: Two-stage acid hydrolysis and the three stage acid hydrolysis. In both cases, the first stage reaction was operated at a temperature of 40 °C and acid concentration of 72 wt.%. The following broad range of reaction conditions were considered for the two stage acid hydrolysis: temperature of the second reactor in the range of 150 to 200 °C, and sulfuric acid concentrations in the range of 4 wt% to 8 wt% for levulinic acid production and 2 wt% to 10 wt% for sugar production. For the three-stage acid hydrolysis, the second stage was operated at a temperature of 121°C and acid concentration of between 2 and 10 wt%; and the third stage was operated at a temperature between 150 and 200 °C and acid concentration between 4 to 8 wt.%. The tested retention times of the final high temperature stage of both routes were 40 min, 80 min, and 120 min. The effect of different reaction conditions was analyzed by Multiway ANOVA.

The glucose production was found to be increased with the temperature and retention time for both the two-stage and three-stage acid hydrolysis. The highest yield of glucose was obtained at 8 wt% of H₂SO₄ concentration. The highest yield of levulinic acid with the two stage hydrolysis was obtained at 200 ° C and for 40 min retention time. However, the highest yield of levulinic acid was obtained at lower acid concentration of 4 wt% with retention time of 80 min with the three-stage acid hydrolysis. The highest yield of levulinic acid based on the weight of sugar kelp was found to be 4.12 wt % with the two-stage acid hydrolysis and 4 wt% with the three-stage acid hydrolysis. These yields of levulinic acid are found to be lower than that of levulinic acid made from woody biomass. Such lower yields can be explained by the low content of hexose presence in the sugar kelp. Additionally, the degradation of glucose to humins may be greater at a high concentration of

acid. Future work is necessary to perform the detailed characterization of ash content of sugar kelp to study its influence on the production of levulinic acid.

CHAPTER 2

2.1 Introduction

Energy conservation is a primary concern for many industrial processes with respect to energy efficiency, product quality and environmental concern. To adjust any process stream to a desired temperature from an ambient condition, or vice versa, there is need for utility systems to deliver heating or cooling capacity to the process through heat exchangers. In big process industries, such as petrochemical industries, multiple streams participate in the processes and operations. This can require large demands of the heating and cooling utility systems to achieve the desired conditions, which increases energy consumption, environmental concerns, and overall economics of the process. Research shows that around 80% of total energy consumption in petrochemical industries is associated with heat transfer (67).

Developing a heat exchanger network using pinch analysis to optimize the process design is a solution to decrease the overall cost of a process. This is achieved by increasing the heat recovery of thermodynamically active streams and by decreasing the utility load from outside. Pinch analysis has been an active area of research for 40 years (68). Currently many models and methods have been developed in an area of process integration and process optimization. Among them pinch technology approach is one of the widest spread and systematic techniques for process integration. In the design of industrial processes, the optimum arrangement of process design can be seen to involve 5 different steps: type of process (batch or continuous process), input and output structure of the process flow diagram, recycle structure of the process, separation units and heat integration/process integration or development of a heat exchanger network (64). The heat exchanger network can be obtained by computing thermodynamically feasible targets in a series of heat exchangers. The concept of pinch technology for heat exchanger network was developed

by Bodo Linhoff and John Flower in 1977 (61). The pinch point is known as a point of zero heat transfer between hot and cold streams. The pinch analysis concept works on the first and second laws of thermodynamics (62). Pinch analysis is a rigorous and graphical approach to determine the energy pockets of any chemical process. The typical savings noted for oil refining, petrochemicals and chemicals are 10-25 %, 15-25 % and 15-35 % respectively, which are expressed based on the total fuel purchase (63).

There are constraints on the matching of surplus and deficit heat streams imposed by the first law (total amount heat transferred in a heat exchanger) and the second law of thermodynamics (direction of heat transfer between hot streams and cold streams). The composite curve is the temperature- enthalpy profile of the process. It is the graphical representation of potential heat transfer opportunities in the system. The minimum temperature difference between hot stream and cold stream (Pinch point) depends upon the value of ΔT_{\min} and this can be fixed by an economic trade off curve (65). Pinch analysis provides the capital and operating costs of the process based on mass and energy balances. The economy of any process is dependent upon the total cost of the process. The total cost can be determined by the economic tradeoff curve, whereby the appropriate value of ΔT_{\min} can be calculated.. A typical value for the optimum value of ΔT_{\min} in a shell and tube heat exchanger is 10 °C (65). Selection of ΔT_{\min} determines the maximum energy recovery, minimum number of heat exchange units and minimum number of heat exchanger networks to optimize the overall cost of the process. The selection of the ΔT_{\min} value also fixes the energy targets of any process. The economy of any process is a function of capital cost and operating cost of the process plant, and both are relevant to the design of heat exchange networks, where capital cost is traded off with utility cost. Based on their heat transfer properties, utilities can be divided into constant temperature and variable temperature utilities. The common types of cold utilities

are cooling water, chilled water and refrigeration systems. Likewise, hot utilities come in forms such as fired heater, hot oil, steam and dowtherm liquid (64). An issue to take into consideration for heat integration of complex chemical processes dealing with multiple chemicals with different physical properties and at different conditions is the use of appropriate materials of construction for pipes and heat exchangers necessary for safety and chemical process considerations.

In this study, I performed pinch analysis and overall cost estimation of a process to convert biomass into thermal deoxygenation oil (TDO oil). The process included the combined acid hydrolysis and dehydration of biomass to levulinic acid and subsequent thermal deoxygenation to produce TDO oil. The process also included separation and recycle of solvents and catalysts. The overall process of developing an energy integration includes five major tasks: (i) selection of streams, (ii) placement of stream matching, (iii) identify the utilities, (iv) calculation of operating cost and capital cost and (v) comparison of cost with energy integration and without energy integration. In addition, the annualized cost of the heat exchangers was the sum of the annualized capital cost of heat exchangers and utilities.

2.1.1 Process Description of Bio-fine process and Thermal Deoxygenation

Combined acid hydrolysis and dehydration and thermal deoxygenation pathway is a renewable fuel technology to convert lignocellulosic feedstock into renewable fuels and chemicals. The TDO process was developed by Professor Wheeler and his research group at Department of Chemical and Biomedical Engineering, University of Maine. In this process, the blended woody biomass undergoes acid hydrolysis and dehydration at 200 °C and 16 bar by diluted sulfuric acid (3-5 wt%) as a catalyst. Cellulose and hemicellulose of woody biomass produces organic acids such as Levulinic acid (LA), formic acid (FA) and furfural (Furf) respectively. Bio-fine char is a byproduct derived from Lignin. The Bio-fine char from the liquid product stream (FA, LA, Furf, Water and

Diluted acid) can be washed and separated by using a series of centrifuges. By burning biochar as boiler fuel, a turbine and generator can produce electricity. Meanwhile the organic acids such as LA and FA can be separated from the mixed stream of water, LA, FA, Furf, and diluted acid in a solvent extraction step making use of 2-methyl tetra hydroxyl furan (MTHF). The solvent can be recovered in a solvent extraction column while the furfural can be purified using a series of distillation columns.

The extracted organic acids go into a neutralization reaction with calcium oxide to form calcium levulinate and calcium formate. These calcium salts of LA and FA undergoes pyrolysis at 450 °C and ambient pressure to produce vapors of TDO oil with a low content of oxygen. Figure 13 outlines the process flow of this system.

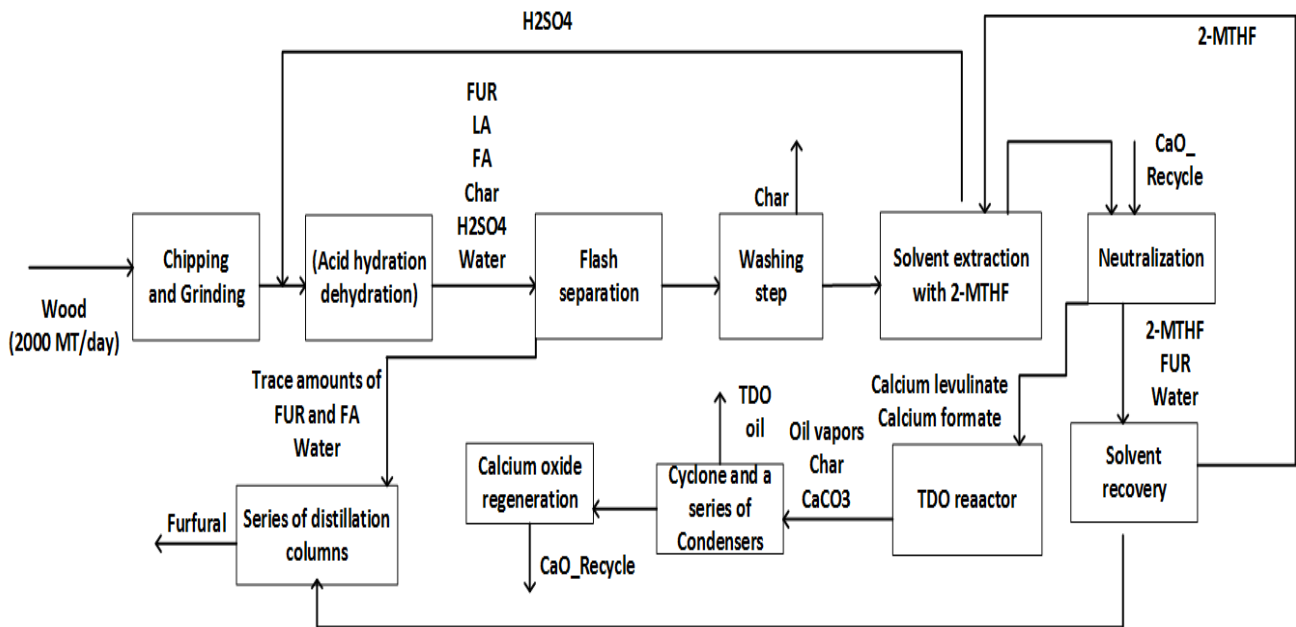


Figure 13 Block Flow Diagram of Combined AHDH and TDO Oil (6)

In this process, the purification and separation of product streams such as LA, FA and furf are dilute streams. Separations require a number of distillation columns and other separation columns, which require a high amount of energy that increases the utility load of the process. Gunukula et al. developed a process model using Aspen Plus simulation. Converting 2000 metric tons of dry wood chips converts into 200 metric tons of TDO oil, 750 tons of biochar with the mass fraction of Furf, LA and FA are 0.04, 0.08, and 0.03 respectively. Aspen plus simulation predicted an energy requirement for the separation and purification of LA and furf are 91 MW and 20 MW respectively (6). The high energy requirements suggest the likely benefit of applying of final stage of process designing, which is known as energy integration or heat exchanger network.

2.2 Materials and Methods

Gunkula et al., used Aspen Plus simulation to simulate and optimize the combined Bio-fine and TDO processes. The material balance of process model was calculated by Aspen Plus simulation. Solid components such as calcium salts of organic acid and char were modeled as non-conventional components. The ENTHGEN method was used to calculate the enthalpy of non-conventional components; and enthalpy of char was calculated by the HCOALGEN enthalpy model (66). After modeling the whole process flowsheet, including recycling and separation, the last step of the process design was energy integration and developing the heat exchanger network.

2.2.1 Data Extraction or Stream Table

Data extraction is an essential part of heat integration / process integration. The combined Bio-fine and TDO process was relatively large, with a total number of streams of more than 60, which could make energy integration very complicated. To simplify the analysis, we considered only the 15 streams with enthalpy flows of more than 1 MW, and which could make heat integration feasible. Additionally, we considered only those streams that did not require any process modification. As

part of the data extraction, we identified all information associated with process streams such as temperature, sensible heat, latent heat, mass flow rate, supply temperature, target temperature and unit operation associated with those streams. Moreover, streams associated with condensers and reboilers were treated independently. Most of the streams in this process were associated with temperature change as well as phase change. We used ASPEN Plus to separate these streams into two different parts: the isothermal stream experiencing phase change and the sensible heat stream going through a temperature change. To facilitate the analysis, isothermal phase change streams were entered into the analysis as undergoing a minor temperature change of 1 °C (increasing for cold streams and decreasing for hot streams). We showed the surplus energy with a negative sign and deficit sign with a positive sign.

2.2.2 Composite Curve/Temperature -Enthalpy Diagram

Composite curve is another way to illustrate the heat transfer between hot streams and cold streams. To produce the composite curve, we produced the shifted temperature curve (Cascade diagram) by considering ΔT_{\min} as 10 °C between hot streams and cold streams. We arranged the temperature of all streams participating in energy integration in descending order. Then we calculated the net energy requirement in each interval by transferring heat from hot streams to cold streams by considering the first and second law of thermodynamics. The net energy balance in each interval was calculated by:

$$Q_{interval} = Q_{sensible} * \left(\frac{\Delta T_{interval}}{\Delta T_{total}} \right)$$

Equation 3 Net energy balance in each interval

Where, $Q_{sensible}$ = total heat available from the hot stream, ΔT_{total} = Inlet and outlet temperature difference of the hot stream, $\Delta T_{interval}$ = temperature difference of the hot stream within the interval.

Moreover, the extra term Q_{latent} was added in above equation for streams associated with latent heat.

$$Q_{interval} = Q_{sensible} * \left(\frac{\Delta T_{interval}}{\Delta T_{total}} \right) + Q_{latent}$$

Equation 4 Net energy balance in each interval factoring in Q_{latent}

Where, Q_{latent} is latent heat duty in temperature interval

We constructed the problem table algorithm (a table which shows net energy requirement in each temperature interval) by taking out an available energy from first temperature interval and the remainder was attributed to the next temperature interval. By doing so, the point in the table where heat transfer was no longer possible between process streams was considered a pinch temperature (4). We produced the composite curve by integrating the heat of hot streams and cold streams in each temperature interval and plotting them on temperature enthalpy diagram in a counter current flow direction. For those intervals in which there is no stream, we showed just a vertical line indicating a change in temperature but no enthalpy change, meaning no heat transfer is available over this temperature range. We moved the hot and cold composite streams in a horizontal manner so as to have both streams touch at one point, which is the pinch point, and that temperature is the pinch temperature.

2.3.3 Grand Composite Curve

A graph of net heat flow against shifted temperature interval is known as the grand composite curve (GCC). It is also known as a residual heat curve, which find the points at which to place an extra utility from outside. As shown in Figure 14, the total heat load from outside is 130.05 MW and the cold utility load from outside is 115.38 MW. In the GCC, the high-pressure steam was used for cold streams at or close to 250 °C, whereas the medium pressure steam and the low-pressure steam took care of cold streams at 212 °C and 134 °C, respectively. Cooling water was

only used as a cold utility requirement because of its certain economic advantages and most streams doesn't need to cool down to 25 °C. Because of different specifications of cooling water with geographic location and weather, we considered 17 °C with room temperature as its specification. For the economics of the process, the penalty for hot utilities was decreased by using the expensive high temperature utility for the highest required temperatures, and then reusing the residual heat, still at a useful temperature, to take care of streams at lower temperature. Moreover, the pockets in the grand composite curve could be used to recover energy for next process stream.

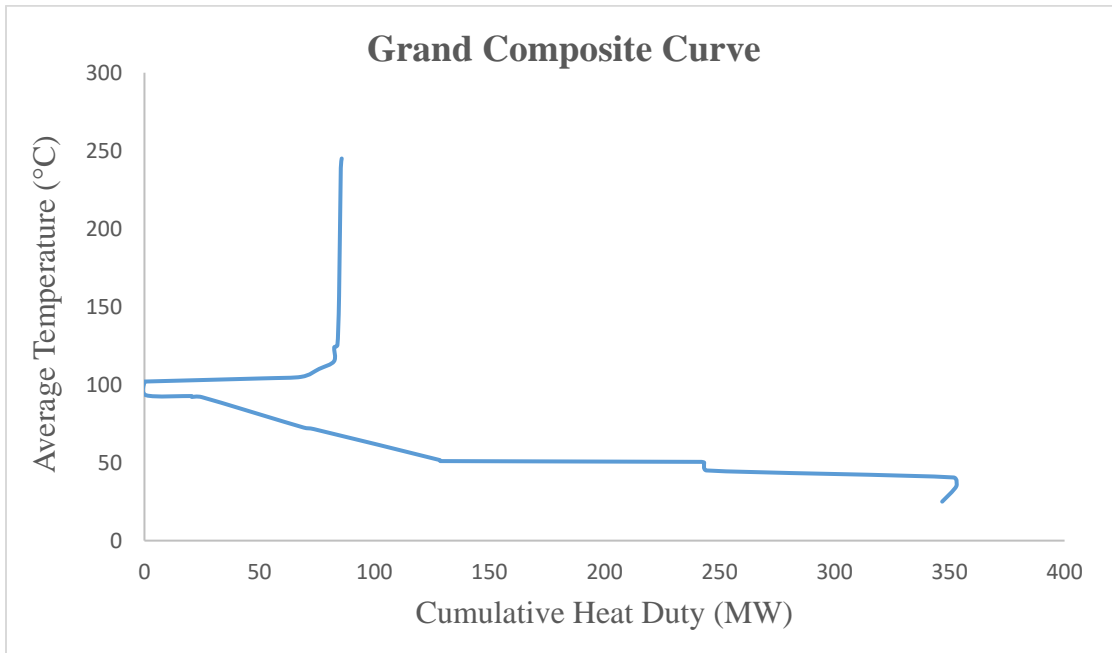


Figure 14 Grand Composite Curve

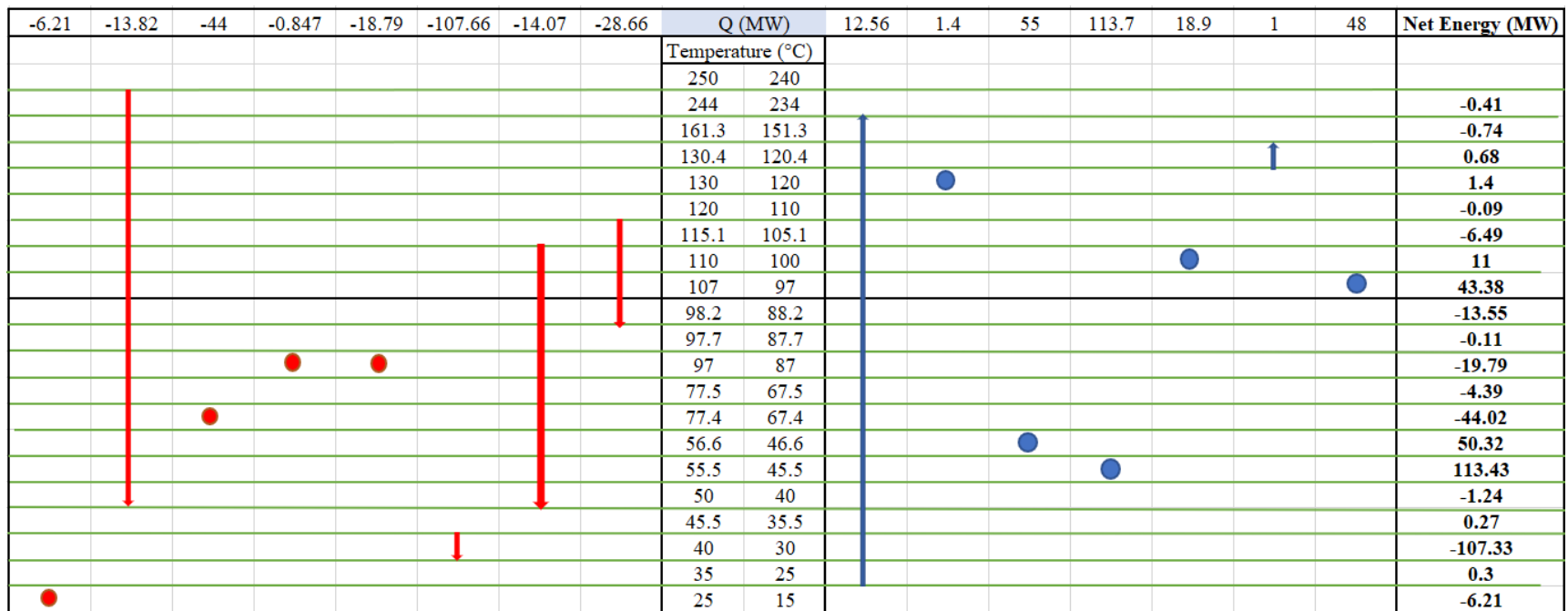


Figure 15 Net Energy Requirement in Each Interval

(the heat duty associated with process streams are expressed in the top row of the figure and vertical lines represent the temperature of hot streams and cold streams at left and right respectively.)

2.2.3 Grand Composite Curve (Residual heat curve)

The graph of net heat flow against shifted temperature interval is known as grand composite curve. Here, we constructed the grand composite curve by considering the net heat surplus and the net heat deficit calculated from the problem table algorithm. We produced the table of cumulative enthalpy (MW) vs average temperature in an interval (°C). For example, we considered average temperature 102°C for an interval in which we had 107 °C for hot the stream and 97 °C for the cold stream. We considered process heat transfer zero at the pinch point and the heat duty at that point was treated as an external hot utility. The cumulative heat duty was calculated at each temperature interval. The equation for cumulative heat duty for sensible heat was:

$$Q_i = \left[\sum \left(\frac{Q_{hot}}{\Delta T_{total}} \right) - \sum \left(\frac{Q_{cold}}{\Delta T_{total}} \right) \right] \Delta T_{interval}$$

Equation 5 Cumulative heat duty for sensible heat

Q_{hot} and Q_{cold} are heat duties of hot streams and cold streams respectively, ΔT_{total} is the initial and final temperature of streams and $\Delta T_{interval}$ is temperature difference at specific interval.

For latent heat the cumulative heat was calculated by:

$$Q_i = \left[\left\{ \sum \left(\frac{Q_{hot}}{\Delta T_{total}} \right) - \sum \left(\frac{Q_{cold}}{\Delta T_{total}} \right) \right\} * \Delta T_{interval} \right] + Q_{latent}$$

Equation 6 Cumulative heat duty for sensible heat factoring in Q_{latent}

Where Q_{latent} is the heat associated with the latent heat stream.

We considered cumulative enthalpy as an independent variable and average temperature as dependent variable. We also placed the hot utilities above pinch and cold utilities below pinch. We considered high pressure steam at (250°C and 40 bar), Medium Pressure steam (212 °C and 20 bar) and Low-pressure steam (134 °C and 3 bar) and cold utility just a cooling water (17 °C and atmospheric pressure).

2.2.4 Placing of Heat Exchangers

After constructing composite curve, grand composite curve and deciding the places of utilities, the next step was to place the matches of streams. We started matching heat surplus and heat deficient streams from the pinch point to make a process simple and more efficient. But we also considered some constraints for placing the matching as illustrated in the algorithms represented in Figure 16 and Figure 17 for the process streams above and below pinch. In this algorithm, N_h and N_c are number of hot streams and cold streams respectively, Q_h and Q_c are heat capacities associated with hot streams and cold streams respectively. After placing the matches, the left-over energy demand was met by using an appropriate utility. For sensible heat streams, the left-over energy was calculated by:

$$Q = m \times C_p \times \Delta T$$

Equation 7 Sensible heat streams left-over energy

Where: m was the mass flowrate stream (tonnes/day), C_p was the specific heat (kJ/kg °C) after transferring the heat, and ΔT was the temperature difference (°C). For streams exchanging latent heat, a heat of vaporization (or condensation) term was added to any streams with an associated phase change. There were some cases in which we needed a stream to match with more than one other stream. To make this feasible, we split that stream into necessary number of streams based on total energy associated with that specific stream. Moreover, we also calculated what the temperature associated with leftover energy stream is by subtracting the heat transfer duty from overall heat duty of the system and temperature was calculated by sensible heat duty and latent heat duty equation.

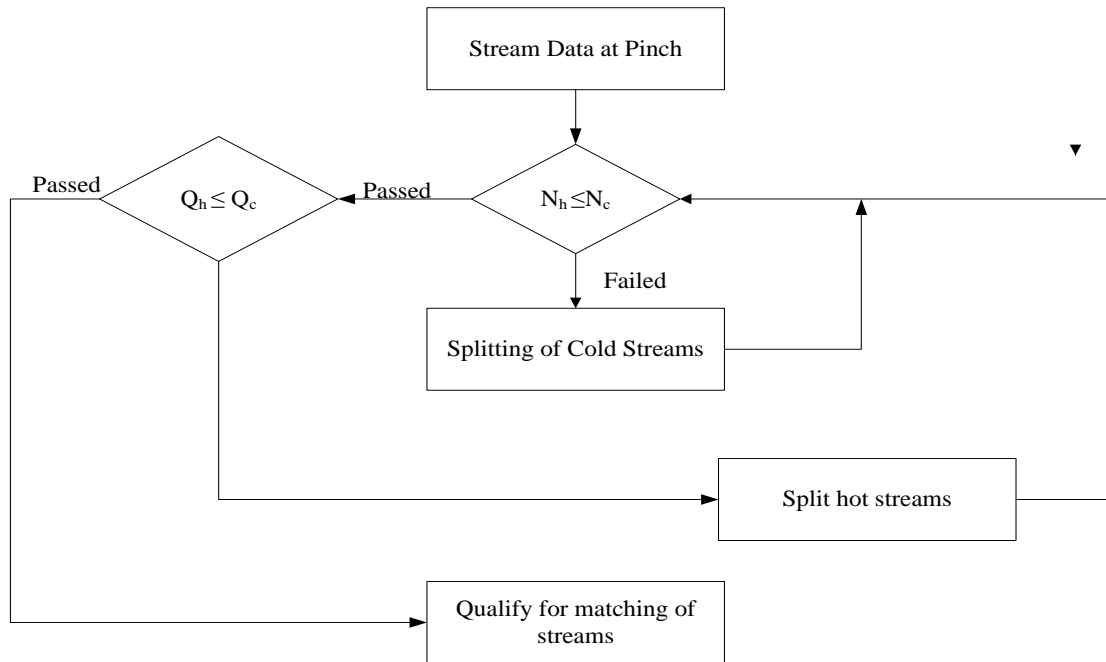


Figure 16 Algorithm for Matching of Streams Above Pinch Region

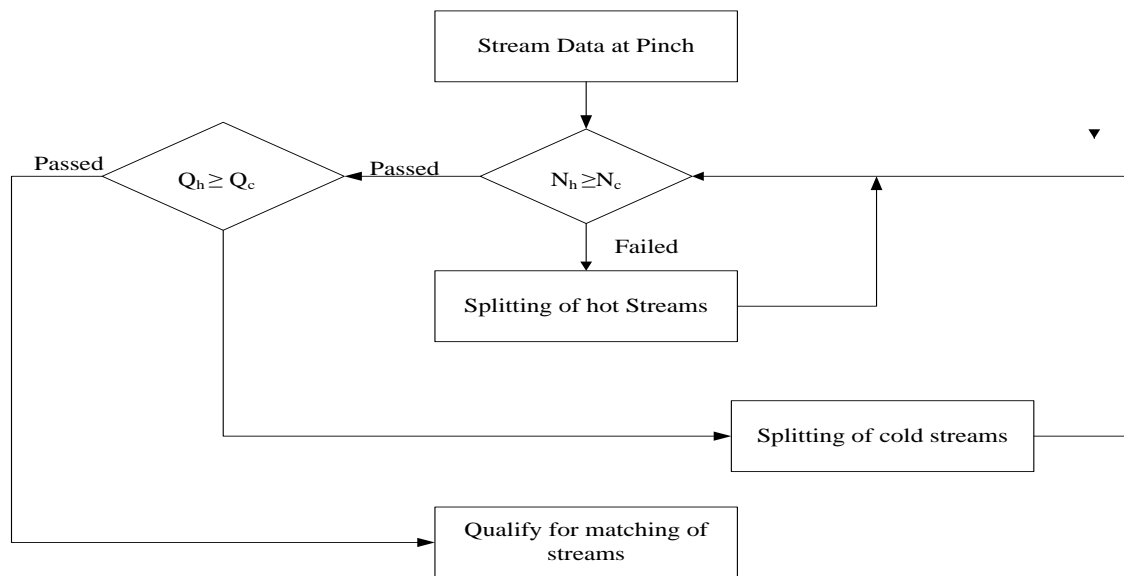


Figure 17 Algorithm for Matching of Streams Below Pinch Region

2.2.5 Area Targeting/Heat Exchanger Network

We constructed a balanced composite curve to calculate the area target in which the overall energy requirement was zero. After placing the matches between hot streams and cold streams and leftover heat was recovered by utilities, the next step was to determine the size of the heat exchangers. We assumed 1-1 shell and tube heat exchanger with pure counter current flow to make the targeted value close to real values of heat transfer and heat exchanger area. The overall heat transfer coefficient U ($\text{w/m}^2\text{°C}$) for different streams was assumed based on Bspang's numbers (69). So, the overall heat transfer area was calculated for the network by:

$$A = \sum_{i=1}^N Q_i / U_i \Delta TLM_i$$

Equation 8 Overall heat transfer area

Where, Q_i is heat duty (kJ/h), U =overall heat transfer coefficient ($\text{w/m}^2\text{°C}$), ΔTLM_i = log mean temperature difference, defined as:

$$\Delta TLM_i = \left[\frac{(T_{hin} - T_{cout}) - (T_{hout} - T_{cin})}{\ln \frac{(T_{hin} - T_{cout})}{(T_{hout} - T_{cin})}} \right]$$

Equation 9 Log mean temperature difference

We placed most of the matches in the Aspen plus simulation to get more precise results and calculates the precise duty associated with specific heat exchangers. Moreover, we only considered sensible heat streams (only in aspen plus simulation) to place the matches for hot streams and cold streams.

2.2.6 Calculation of Heat Exchanger Area in ASPEN Plus

Overall heat transfer coefficient (U) of process streams was taken from Bspang's number (69). We considered hot fluid on the shell side and cold fluid on the tube side. We placed the heat exchangers in the flow sheet, connected streams in countercurrent flow directions and considered different specifications such as minimum temperature difference and specific known stream outlet temperature to calculate the heat transfer areas. By using the thermal results and by conditioning in rating mode, we calculated the outlet temperature of streams and percentage of oversized or undersized systems (kept to within a limit of up to 20%) We compared the Aspen results of area with the results from the spreadsheet calculations to note the difference in results of heat exchanger area calculations.

2.2.7 Cost Estimation

2.2.7.1 Utility Cost Calculation

The total annual cost of heat exchanger network predicts the nature of capital cost, operating cost and minimum temperature difference base on tradeoff curve. Operating cost, in other words utility cost, is a function of inflation and energy cost. Manufacturing cost was derived from labor cost and the Chemical engineering plant cost Index (CEPCI). We used a two factor utility cost equation:

$$C_{s,u} = a(\text{CEPCI}) + b(C_{s,f})$$

Equation 10 Utility Cost

where, $C_{s,u}$ is the price of utility, a and b are utility cost coefficients, $C_{s,f}$ is the price of fuel in \$/GJ (10). We used Bio-fine char as our fuel and tap water as our cooling supply. Prices for these sources were 52.50 \$/GJ (AMEC report for sustainable energy report) and \$ 0.067 per 1000 kg (\$0.03 per GJ, by considering a heat of vaporization of water as 40.65 kJ/mol) (73).

For the steam utility, we considered factor “a” for a process module was

$$a = 2.7 \times 10^{-5} m_s^{-0.9}$$

where $0.06 < m_s < 40$ kg/s and factor “b” was

$$b = 0.0034 p^{0.05}$$

where, the values of p lie between 1 to 46 barg (10).

For cooling water, we calculated the price of water in $\$/m^3$. Here, factor a was calculated as:

$$a = 1.0 \times 10^{-4} + 3 \times 10^{-6} q^{-0.6}$$

Equation 11 Price of tap water

where q was the flowrate of water for which the value lies between 0.01 and 10 m^3/s and factor b was 0.003. The process streams and utility streams were matched in ASPEN Plus and those results were used to calculate an annual price of utility. Moreover, for unit R 401 on the flow sheet (Precipitator), the inlet and outlet temperatures of process streams were 670 °C to 50 °C, so tap water was used as a cold utility. The specifications for cooling water were: heat of vaporization= 40.65 kJ/mol, mass flow of water was 957269 kg/day and the price was \$ 21,165 per year by considering 330 operating days) taken from Pearson 4th edition. For R-402 (TDO reactor) the process stream goes from 250°C to 450 °C so, natural gas used as a hot utility at 460 °C, (Specification were density= 0.715 kg/nm³, Higher heating value= 38.01 kg/Nm³) (74) the price was \$ 8.2 per million BTU (from US energy department).

2.2.7.2 Installed Cost Calculation

We calculated an installed cost of heat exchanger by calculating an area of heat exchanger and material of construction of specific process streams was considered from Pearson Chapter 7 (74).

We calculated an installed cost of heat exchangers in 1990 from exchanger cost per area ($\$/ft^2$)

(Fixed tube heat exchanger) and different materials of construction (72) (73). We calculated an installed cost in 2016 by using index cost of 2016 (inflation condition) (585) and 1990 (357.6).

The equation was:

$$\text{Installed cost of heat exchanger in 2016} = \text{installed cost in 1990} * \left(\frac{\text{Cost Index in 2016}}{\text{Cost Index in 1990}} \right)$$

Equation 12 Installed cost of heat exchanger in 2016

The installed cost of heat exchangers was the cost of heat exchanger multiplied by a cost factor (2.2, which includes labor charge, transportation, and other expenses to fix the heat exchanger).

The CEPCI includes equipment, pipes, valves, fitting, fabrication, maintenance equipment.

2.2.7.3 Capital Cost of Estimation

Capital cost of heat exchangers was the sum of the direct cost and indirect cost of heat exchangers.

The direct cost of heat exchangers included equipment cost, raw material cost, warehouse, additional pipes and fittings. Indirect cost included administrative cost, tax, labor expenses, and field expenses. Installed cost of heat exchanger was multiplied by 2.5 to give the capital cost of heat exchangers (75).

2.2.7.4 Total Annualized Cost

Total annualized cost was the sum of annualized capital cost per year and annualized cost of utilities. Total annualized capital cost was the function of capital cost of heat exchange and annualized capital cost per year. Annualized capital cost was calculated by:

$$\text{Annualized capital cost} \left(\frac{A}{Pr}, n \right) = r * \frac{(1 + r)^n}{(1 + r)^n - 1}$$

Equation 13 Annualized capital cost

where, r= interest rate per year= 20% and n= number of years=30 years (plant life).

2.3 Results and Discussion

2.3.1 Data Extraction

The key information of the data extraction step is to identify the temperature levels of the streams and amount of heat required for those process streams to reach a desired temperature level. We assumed that most process streams are in a single phase (by treating sensible heat duty and latent heat duty differently) and the energy associated with those phases was considered for further steps of energy integration. Furthermore, applying a small token temperature change in the outlet temperature for the latent heat streams doesn't make a significant difference in the analysis. Specific heat is a nonlinear function of temperature. After considering all heuristics for data extraction, we came up with the energy requirement for the cold streams of 250 MW and the energy available the hot streams were 234 MW. So, based on the first law of thermodynamics a minimum of 16 MW should be supplied from the outside hot utility in the absence of any further constraints.

Table 12 Data Extraction for Energy Integration

Unit Operation	Stream Number	Stream Type	Tin (°C)	Tout (°C)	Q (MW)	Mass Flow (Tonnes/day)	Block	Sensible Heat (MW)	Latent Heat (MW)
Heater	105-106	Cold	25	234	12.56	396.33	E101	4.37	8.21
Flash Separator	107-108,111	Cold	119	120.1	1.4	6040.68	E102		1.4
Evaporator	Sulfr, Sulfr1, Waste water	Cold	46	46.6	55	4308.81	EW101		55
Evaporator	918-917, 301 B	Cold	45	45.5	113.7	8125.48	E107		113.68
Distillation column reboiler	112,112 B, Furf1- Waste water	Cold	99	100.1		1209.91	DS-101		18.85
Distillation column reboiler	112 C- Purefurf	Cold	120.4	151.3	1	236.47	DS-102	1	
Distillation column reboiler	912-FURD	Cold	97	97.1	48	261	DS-103		48
Condenser	111-112	Hot	120	98.2	-28.66	1184.89	E103A	0.2848	28.1452
Condenser	917-920	Hot	45.5	40	-107.7	4118.87	E106	0.4481	107.623
Distillation column Condenser	112,112 B, FURD 1- 112 A	Hot	97.7	97.1	-18.79	857.52	DS-101	-1.97	16.82
Distillation column Condenser	112 C-112 D	Hot	97.7	97	-0.847	42.1	DS-102		0.93
Distillation column Condenser	912-916	Hot	77.5	77.4	-44	4827.28	DS-103		-44
Condenser	419-420,421,422	Hot	25	25	-6.21	325.51	V402		-6.21

2.3.2 Composite Curve

The problem table algorithm was used to calculate the net energy in each temperature interval for pinch analysis. Represented results from the problem table algorithm show that after transferring heat in each temperature interval, the total hot utility requirement was 130.60 MW and the cold utility requirement was 114.21 MW (Considering heat duty requirement of 43.38 MW at the pinch point). The difference between two utility requirements was 16.39 MW which confirms the initial first law calculation. In addition, for physical interpretation of heat transfer, the cold composite curve should be below the hot composite curve fulfilling the second law of thermodynamics. The total heat transfer at the pinch point should be zero but following the same heat duties from cascade diagram doesn't follow constraints (there is 43.38 MW heat transfer at 107 °C and 97 °C between hot streams and cold streams respectively). To keep the cold composite curve on the right side of the diagram, 20 MW (heat duty at pinch temperatures of hot streams and cold streams) is the minimum hot utility added when considering that the change in total specific heat capacity of all the cold streams is constant. In addition, the overlap of hot and cold streams shows non-feasibility of heat transfer. The net hot utility requirement is now 37.56 MW and cold utility requirement remains 24.90 MW after transferring heat between hot streams and cold streams. Figure 19 shows the resulting balanced composite curve. It shows the places of hot utility and cold utility on temperature-enthalpy diagram.

Table 13 Cumulative Heat Duty of Hot Streams and Cold Streams in Temperature Intervals

Heat Duty for Hot Streams (MW)	Hot Stream Temperature (°C)	Cold Stream Temperature (°C)	Heat Duty for cold Streams (MW)
0.00	24.90	-	-
6.21	25.00	-	-
6.21	35.00	-	-
6.21	40.00	30.00	37.30
113.87	45.50	35.50	37.63
115.16	50.00	40.00	37.90
116.58	55.00	45.00	38.20
116.72	55.50	45.50	151.93
116.87	56.00	46.00	151.96
117.04	56.60	46.60	207.00
122.72	76.50	66.50	208.19
167.00	77.50	67.50	208.25
172.56	97.00	87.00	209.43
172.71	97.10	87.10	209.43
192.40	97.70	87.70	209.47
193.20	98.20	88.20	209.50
207.24	107.00	97.00	210.03
207.40	107.10	97.10	258.03
210.43	109.00	99.00	258.15
212.02	110.00	100.00	277.11
220.13	115.08	105.08	277.41
226.91	120.00	110.00	277.71
227.54	129.00	119.00	278.25
227.63	130.40	120.40	279.73
229.77	161.30	151.30	282.59
235.48	244.00	234.00	287.56
235.90	250.00	240.00	287.56

Table 14 Table for Grand Composite Curve

Hot Utility Requirement From outside (MW)	Heat Cascade (MW)	Cumulative Duty in each interval (MW)	Average Temperature Interval (°C)	Heat Transfer in each interval (MW)
	0.41	0.41	245.00	85.77
	1.15	0.74	239.00	85.35
	0.43	-0.72	156.30	84.61
0.95	0.00	-1.39	125.40	83.89
	0.08	0.08	124.00	82.50
	6.57	6.49	115.00	82.42
	14.37	7.80	110.08	75.93
3.00	0.00	-17.36	105.00	68.13
	2.92	2.92	104.00	50.76
44.93	0.00	-47.85	102.00	0
	13.51	13.51	102.00	0.00
	14.28	0.77	93.20	0.77
	33.93	19.65	92.70	20.42
	34.07	0.14	92.10	20.56
	38.46	4.39	92.00	24.95
	82.69	44.23	72.50	69.18
	87.17	4.48	71.50	73.66
	32.31	-54.86	51.60	128.53
	32.42	0.11	51.00	128.64
81.17	0.00	-113.59	50.50	242.23
	1.13	1.13	50.00	243.35
	2.14	1.01	45.00	244.36
	109.47	107.33	40.50	351.70
	109.17	-0.30	35.00	353.00
	115.38	6.21	25.00	346.79

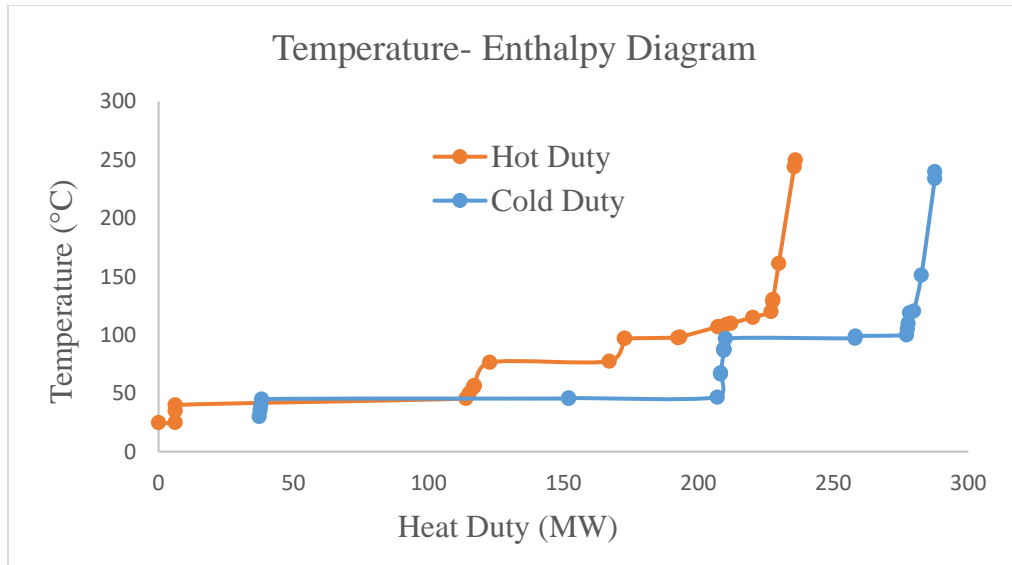


Figure 18 Composite Curve

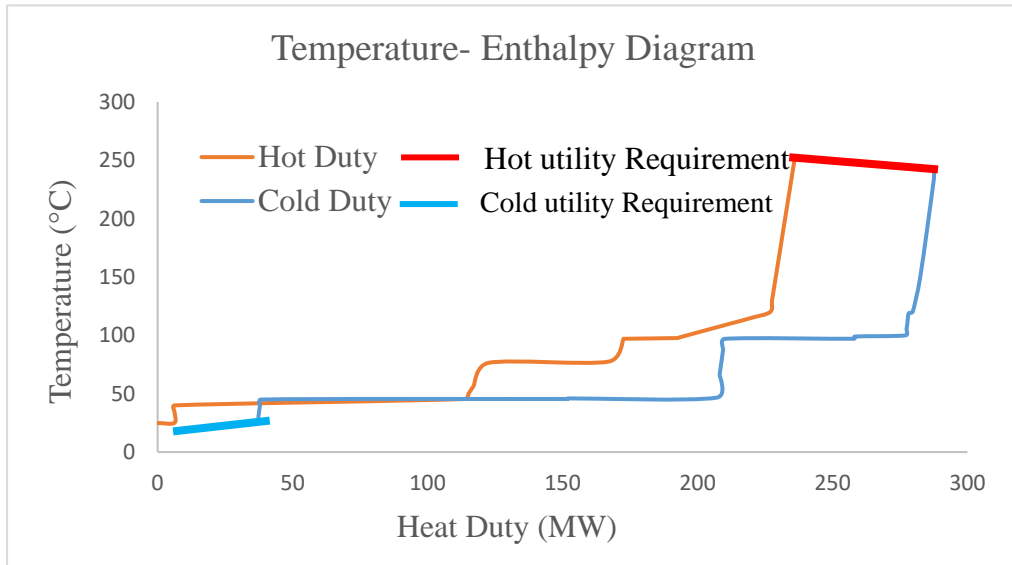


Figure 19 Balanced Composite Curve

2.3.4 Area Targeting Network

Figure 20 shows the complete minimum energy design of heat exchanges with matching of hot streams and cold streams above and below pinch. Moreover, the mixture of sensible heat and latent heat streams makes the process more complex, and certain pressure drops also create some

problems in pinch analysis. All in all, considering an appropriate heat transfer coefficient for process streams and matching sensible heat streams with temperature changing streams makes the process more feasible. We matched the sensible heat streams in Aspen plus by considering the pressure drop to be zero while in the heat transfer phase, however in reality under latent heat conditions, heat transfer between streams does create certain pressure changes. The matching of latent heat streams with hot utility streams caused a very small amount of pressure drop and temperature change of the utility streams, but this did not create any modification in process streams. This could be one of the reasons for the non-identical utility requirement for the composite curve and the grand composite curve. The selection of a 1-1 shell and tube heat exchanger could need a lower surface area for heat transfer compared to a 1-2 or a 2-4 shell and tube heat exchanger. The total area requirement of 1-1 shell and tube heat exchangers was 23,808 m². Whereas, without energy integration the area of heat exchangers was 20,728 m². The results of heat exchanger area and matching of process streams and utility streams are shown in Table 15.

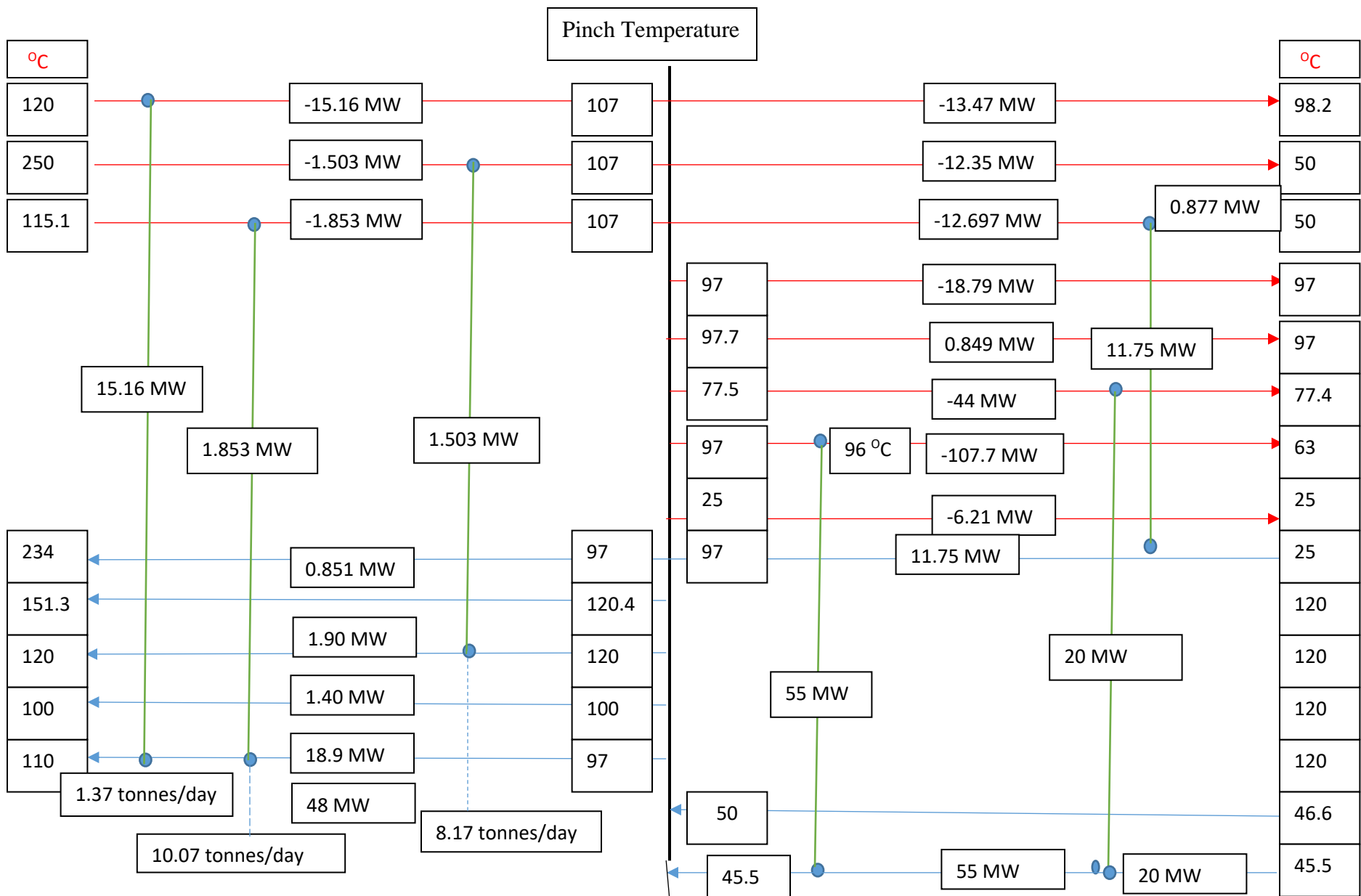


Figure 20 Complete Minimum Energy Design

Table 15 Stream Matching and Heat Exchanger Area

Heat exchanger	U (watt/m ² °C)	Heat Duty (MW)	T _{cin} (°C)	T _{cout} (°C)	T _{hin} (°C)	T _{hout} (°C)	Type of Utility	Heat exchanger area (m ²)
HE-01	900	15.16	97.0	100.2	120.0	107.0	-	1072
HE-02	900	1.50	100.2	104.7	250.0	114.0	-	50
HE-03	900	1.85	104.7	110.0	115.1	107.0	-	1470
HE-04	300	0.88	25.0	97.0	107.0	54.0	-	4425
HE-05	350	55.00	46.6	52.2	97.0	96.8	-	3311
HE-06	850	20.00	45.5	45.9	97.0	96.7	-	1117
HE-07	850	0.85	97.0	234.0	250.0	250.0	HPS	250
HE-08	850	1.40	120.0	120.1	134.0	134.0	LPS	118
HE-09	850	18.84	100.0	107.0	134.0	133.6	LPS	1854
HE-10	850	1.90	120.4	151.3	212.0	212.0	MPS	840
HE-11	850	13.47	17.0	59.0	107.0	97.0	CW	762
HE-12	850	12.34	17.0	40.8	107.0	50.0	CW	863
HE-13	850	0.88	17.0	17.0	54.0	50.0	CW	840
HE-14	850	18.74	17.0	17.0	97.7	97.4	CW	775
HE-15	850	0.80	17.0	17.0	97.7	97.0	CW	33
HE-16	850	44.17	17.0	17.0	77.5	74.0	CW	2507
HE-17	850	32.50	17.0	17.0	96.7	64.0	CW	1765
HE-18	850	6.21	15.0	17.0	25.1	25.0	CW	810
HE-19	850	29.48	97.0	97.7	134.0	134.0	LPS	946

2.3.5 Cost Targeting

The goal of the heat exchanger network synthesis was to minimize to total cost of the network by minimizing the operating and capital costs of the heat exchangers. According to the tradeoff curve, there is a tradeoff between operating cost and capital cost of the heat exchangers at certain minimum temperature difference. So, the overall cost targeting is divided into two parts: (1) Capital Cost of heat exchangers and (2) Utility Cost.

2.3.6 Capital Cost of Heat Exchangers

Capital cost and operating cost of heat exchangers are expressed in different term basis. Thus, it is necessary to be expressed in the same term basis. Annualized capital cost is an equation to convert the capital cost in the same unit period as utility cost. Moreover, for the different types of materials of construction and heat transfer coefficients also change the cost of the heat exchanger so, purchased cost vs Surface area graph from Peters and Timmerhaus helps to provide consistency of cost of heat exchangers for different materials of construction (76). Different material of construction for different heat exchangers was obtained from Sandler and Luckiewicz (77). By considering factor 2.2 to convert heat exchanger price to installed cost (considering labor, suppliers, maintenance and repairs and general expenses), the installed costs of heat exchangers in the cases of energy integration or without energy integration were \$5,103,732 and \$ 4,963,372, respectively (the calculation of each heat exchanger is shown in Table 16). The final capital costs of the heat exchangers were \$ 12,759,330 and \$ 12,408,428 for the cases of energy integration and without energy integration, respectively. Table 16 shows the purchased cost and installed of heat exchangers.

Table 16 Purchased and Installed Costs of Heat Exchangers

Heat exchanger	T _{cin} (°C)	T _{cout} (°C)	T _{hin} (°C)	T _{hout} (°C)	Area (m ²)	Area (ft ²)	Purchased Cost in 1990 (\$)	Purchased Cost in 2016 (\$)	Installed Cost in 2016 (\$)
HE-01	97.0	100.2	120.0	107.0	1072	11534	67,000	109,606	241,133
HE-02	100.2	104.7	250.0	114.0	32	339	7000	11,451	25,193
HE-03	104.7	110.0	115.1	107.0	146.59	1578	15,400	25,193	55,424
HE-04	25.0	97.0	107.0	54.0	4425.05	47631	248,000	405,705	892,550
HE-05	46.6	52.2	97.0	96.8	3310.73	35636	186,000	304,279	669,413
HE-06	45.5	45.9	97.0	96.7	1117	12025	69,000	112,878	248,331
HE-07	97.0	234.0	250.0	250.0	14	150	4,500	7,362	16,195
HE-08	120.0	120.1	134.0	134.0	334.52	3600.84	12,000	19,630	43,187
HE-09	100.0	107.0	134.0	133.6	1854.33	19960	102,000	166,862	367,097
HE-10	120.4	151.3	212.0	212.0	84.30	907	17,000	27,810	61,183
HE-11	17.0	59.0	107.0	97.0	761.98	8202	48,000	78,523	172,752
HE-12	17.0	40.8	107.0	50.0	862.68	9286	50,000	81,795	179,950
HE-13	17.0	17.0	54.0	50.0	83.79	902	11,000	17,995	39,589
HE-14	17.0	17.0	97.7	97.4	775.14	8344	41,000	67,072	147,559
HE-15	17.0	17.0	97.7	97.0	33.09	356	6,200	10,143	22,314
HE-16	17.0	17.0	77.5	74.0	2506.53	26980	144,000	235,570	518,255
HE-17	17.0	17.0	96.7	64.0	1764.55	18993	102,000	166,862	367,097
HE-18	15.0	17.0	25.1	25.0	2296	24711	134,000	219,211	482,265
HE-19	97.0	97.7	134.0	134.0	2682	28865	154,000	251,930	554,245

2.3.7 Operating Cost of Heat Exchangers

Utility costs basically depend upon on the Chemical Engineering Plant Cost index and fuel cost. In the utility cost calculation equation (equation 11) “a” is dependent upon plant size (74). If plant capacity is higher than the utility cost per product volume will be lower. Coefficient “b” depends upon the price of fuel and includes turbine, generator and other equipment used to produce hot pressurized utility systems to regenerate the utility or electricity. The annual utility cost of heat exchangers was \$ 12,332,872 and \$ 16,713,256 for the process with energy integration and without energy integration, respectively. In this process, around 94.40 MW of utility duty was covered by process stream matching, which adds an impetus for utility savings of this process. Hence the hot and cold utility requirements for process integration were 52.48 MW and 129.09 MW respectively. However, in the case of process without integration, the utility requirements were 128 MW and 151 MW hot utility and cold utility requirements, respectively. In both the cases, the cost of high-pressure steam and medium pressure steam were the same (\$ 659,009 and \$ 479,375 for high pressure steam and medium pressure steam respectively), but the use of low-pressure steam and cooling water were higher in the case of process without energy integration, which made a noticeable change in the utility cost of the process (35 % of cost saving from low pressure steam and 54 % cost savings with tap water). Table 17 shows the annual utility cost of heat exchangers and mass flow of utility streams.

Table 17 Annual Utility Costs (Operating days per year:330)

Type of Utility	Thermodynamic Conditions		Without Energy Integration		With Energy Integration	
	Pressure (bar)	Temperature (°C)	Mass flow (kg/h)	Annual Utility Cost (\$)	Mass flow (kg/h)	Annual Utility Cost
High Pressure Steam	40	250	2665	660,528	2665	660,528
Medium Pressure Steam	20	212	3624	479,375	3623	479,375
Low Pressure Steam	3	135	203505	16,848,018	83124	11,022,060
Cooling Water	0.01	17	380274	369,928	188044	170,149
Natural Gas			541.75	976,588	541.75	976,588

2.3.8 Total Cost of Heat Exchangers

The total cost of the heat exchanger is the main tradeoff between utility cost and fixed cost of the heat exchangers. The fixed cost of heat exchangers depends upon life period of heat exchangers. So, both costs are added by considering the time span for a year. Total annualized cost of capital is \$2,492,185 in the case of without energy integration. But it was 3 % higher in the case of energy integration. The total annual cost of heat exchangers was \$ 15 million and \$ 19 million for the process with energy integration and the process without energy integration. Table 18 compares the total annual cost of heat exchangers with energy integration and without energy integration.

Table 18 Cost Comparison of Heat Exchangers

	Cost Without Energy Integration (\$MM)	Cost with Energy Integration (\$MM)
Installed Cost of Heat Exchangers	\$4.96	\$5.1
Capital Cost of Heat Exchangers	\$12.40	\$12.76
Cost of Capital per year	\$2.50	\$2.56
Total annual Cost of Utilities	\$16.52	\$12.33
Total Annualized Cost	\$19.04	\$14.89

2.4 Conclusion

In conclusion, pinch analysis technique was used to calculate the external utility requirements for the Combined Bio fine and TDO oil process, with the optimum heat exchange temperature difference considered as 10 °C. After placing of matches, the hot and cold utility requirements with energy integration are 52.48 MW and 129 MW, respectively, and 94.40 MW of heat duty can be covered from the matching of process streams by considering pinch analysis optimization. It means that 34.2 % of the total heat duty was covered by matching the process streams, resulting in savings of around 26% of external heat load, improving the economy of the process. However, the increase in capital cost doesn't have a big effect on the total cost of the process. The heat energy loss adds to the weight of energy cost by considering both the external utility consumption and the internal energy loss in the heat exchanger network. It benefits from heat recovery and energy conservation at the comparatively lower cost of higher area in the heat exchange network and capital investment. The tradeoff between capital and operating cost was also true for this process. The overall cost saving can be reached up to 22 % with pinch analysis. This overall cost saving is in the range of typical cost savings achieved by the petrochemical and chemical industries (63). It is A green process because it requires only 60% of the bio char to produce the electricity of hot utility.

BIBLIOGRAPHY

1. International Energy Agency <https://www.eia.gov/totalenergy/data/annual/pdf/aer.pdf>
2. U.S. Department of Energy (2011). U.S. Billion-Ton Update: Biomass Supply for a Bioenergy and Bioproducts Industry. R.D. Perlack and B.J. Stokes (Leads), ORNL/TM-2011/224. Oak Ridge National Laboratory, Oak Ridge, TN. 227p.
3. United States EPA- Renewable Fuel Standard (RFS) <https://www.epa.gov/renewable-fuel-standard-program/overview-renewable-fuel-standard>
4. McKendry, P. (2002). Energy production from biomass (part 2): conversion technologies. *Bioresource technology*, 83(1), 47-54.
5. Williams, P. T., & Besler, S. (1996). The influence of temperature and heating rate on the slow pyrolysis of biomass. *Renewable energy*, 7(3), 233-250.
6. Mihalcik, D. J., Mullen, C. A., & Boateng, A. A. (2011). Screening acidic zeolites for catalytic fast pyrolysis of biomass and its components. *Journal of Analytical and Applied Pyrolysis*, 92(1), 224-232.
7. Carlson, T. R., Jae, J., Lin, Y. C., Tompsett, G. A., & Huber, G. W. (2010). Catalytic fast pyrolysis of glucose with HZSM-5: the combined homogeneous and heterogeneous reactions. *Journal of Catalysis*, 270(1), 110-124.
8. Asadullah, M., Ito, S. I., Kunimori, K., & Tomishige, K. (2002). Role of catalyst and its fluidization in the catalytic gasification of biomass to syngas at low temperature. *Industrial & Engineering Chemistry Research*, 41(18), 4567-4575.
9. Zhang, Y., Brown, T. R., Hu, G., & Brown, R. C. (2013). Techno-economic analysis of two bio-oil upgrading pathways. *Chemical Engineering Journal*, 225, 895-904.
10. Gollakota, A. R. K., Kishore, N., & Gu, S. (2017). A review on hydrothermal liquefaction of biomass. *Renewable and Sustainable Energy Reviews*.
11. Bridgwater, A. V. (1994). Catalysis in thermal biomass conversion. *Applied Catalysis A: General*, 116(1-2), 5-47.
12. Bioenergy Consult- biochemical conversion technologies
<https://www.bioenergyconsult.com/biochemical-conversion-technologies/>
13. Milledge, J. J., Smith, B., Dyer, P. W., & Harvey, P. (2014). Macroalgae- derived biofuel: a review of methods of energy extraction from seaweed biomass. *Energies*, 7(11), 7194-7222.

14. Rowbotham, J. S., Dyer, P. W., Greenwell, H. C., Selby, D., & Theodorou, M. K. (2013). Copper (II)-mediated thermolysis of alginates: a model kinetic study on the influence of metal ions in the thermochemical processing of macroalgae. *Interface focus*, 3(1), 20120046.
15. Meinita, M. D. N., Hong, Y. K., & Jeong, G. T. (2012). Detoxification of acidic catalyzed hydrolysate of *Kappaphycus alvarezii* (cottonii). *Bioprocess and biosystems engineering*, 35(1-2), 93-98.
16. The U.N. department of economics and affairs
<https://www.un.org/development/desa/en/news.html>
17. U.S. Department of Energy Efficiency and Renewable Energy
<https://www.nrel.gov/docs/fy04osti/35523.pdf>
18. Bio based Industries Consortium <https://biconsortium.eu/library/case-studies/levulinic-acid-production>
19. Muranaka, Y., Suzuki, T., Sawanishi, H., Hasegawa, I., & Mae, K. (2014). Effective production of Levulinic acid from biomass through pretreatment using phosphoric acid, hydrochloric acid, or ionic liquid. *Industrial & Engineering Chemistry Research*, 53(29), 11611-11621.
20. Xiao-an, W. Y. G. N., & Zhen-xing, L. I. U. Study on Preparation of Levulinic acid from Biomass and its Prospects.
21. Yan, K., Jarvis, C., Gu, J., & Yan, Y. (2015). Production and catalytic transformation of Levulinic acid: A platform for specialty chemicals and fuels. *Renewable and Sustainable Energy Reviews*, 51, 986-997.
22. McKenzie, B. F. (1929). *Organic Syntheses* (IX).
23. Mascal, M., & Nikitin, E. B. (2010). High-yield conversion of plant biomass into the key value-added feedstocks 5-(hydroxymethyl) furfural, Levulinic acid, and levulinic esters via 5-(chloromethyl) furfural. *Green Chemistry*, 12(3), 370-373.
24. Thomas, R. W., & Schuette, H. A. (1931). Studies on Levulinic acid. I. Its preparation from carbohydrates by digestion with hydrochloric acid under pressure. *Journal of the American Chemical Society*, 53(6), 2324-2328.
25. Peng, L., Lin, L., Zhang, J., Zhuang, J., Zhang, B., & Gong, Y. (2010). Catalytic conversion of cellulose to Levulinic acid by metal chlorides. *Molecules*, 15(8), 5258-5272.
26. Carlson, L. J. (1962). U.S. Patent No. 3,065,263. Washington, DC: U.S. Patent and Trademark Office.

27. Chang, C., Xiaojian, M. A., & Peilin, C. E. N. (2006). Kinetics of Levulinic acid formation from glucose decomposition at high temperature. *Chinese Journal of Chemical Engineering*, 14(5), 708-712.
28. Salak Asghari, F., & Yoshida, H. (2006). Acid-catalyzed production of 5-hydroxymethyl furfural from D-fructose in subcritical water. *Industrial & Engineering Chemistry Research*, 45(7), 2163-2173.
29. Redmon, B. C. (1956). U.S. Patent No. 2,738,367. Washington, DC: U.S. Patent and Trademark Office.
30. Efremov, A. A., Pervyshina, G. G., & Kuznetsov, B. N. (1998). Production of Levulinic acid from wood raw material in the presence of sulfuric acid and its salts. *Chemistry of natural compounds*, 34(2), 182-185.
31. Lourvanij, K., & Rorrer, G. L. (1997). Reaction Rates for the Partial Dehydration of Glucose to Organic Acids in Solid-Acid, Molecular-Sieving Catalyst Powders. *Journal of Chemical Technology & Biotechnology: International Research in Process, Environmental AND Clean Technology*, 69(1), 35-44.
32. Wiggins, L. F. (1949). The utilization of sucrose. In *Advances in Carbohydrate Chemistry* (Vol. 4, pp. 293-336). Academic Press.
33. Girisuta, B., Janssen, L. P. B. M., & Heeres, H. J. (2007). Kinetic study on the acid-catalyzed hydrolysis of cellulose to Levulinic acid. *Industrial & engineering chemistry research*, 46(6), 1696-1708.
34. Efremov, A. A., Pervyshina, G. G., & Kuznetsov, B. N. (1997). Thermocatalytic transformations of wood and cellulose in the presence of HCl, HBr, and H₂SO₄. *Chemistry of natural compounds*, 33(1), 84-88.
35. Serrano-Ruiz, J. C., Braden, D. J., West, R. M., & Dumesic, J. A. (2010). Conversion of cellulose to hydrocarbon fuels by progressive removal of oxygen. *Applied Catalysis B: Environmental*, 100(1-2), 184-189.
36. Deng, L., Li, J., Lai, D. M., Fu, Y., & Guo, Q. X. (2009). Catalytic conversion of biomass-derived carbohydrates into γ -valerolactone without using an external H₂ supply. *Angewandte Chemie*, 121(35), 6651-6654.
37. Mascal, M., & Nikitin, E. B. (2009). Dramatic advancements in the saccharide to 5-(chloromethyl) furfural conversion reaction. *ChemSusChem: Chemistry & Sustainability Energy & Materials*, 2(9), 859-861.

38. Yan, L., Yang, N., Pang, H., & Liao, B. (2008). Production of Levulinic acid from bagasse and paddy straw by liquefaction in the presence of hydrochloride acid. *CLEAN–Soil, Air, Water*, 36(2), 158-163.
39. Dunlop, A. P., & Wells, J. P. A. (1957). U.S. Patent No. 2,813,900. Washington, DC: U.S. Patent and Trademark Office.
40. Ghorpade, V. M., & Hanna, M. A. (1999). U.S. Patent No. 5,859,263. Washington, DC: U.S. Patent and Trademark Office.
41. Fitzpatrick, S. W. (1997). U.S. Patent No. 5,608,105. Washington, DC: U.S. Patent and Trademark Office.
42. Fahmi, R., Bridgwater, A. V., Darvell, L. I., Jones, J. M., Yates, N., Thain, S., & Donnison, I. S. (2007). The effect of alkali metals on combustion and pyrolysis of Lolium and Festuca grasses, switchgrass and willow. *Fuel*, 86(10-11), 1560-1569. (42) Determination of total solids in biomass and total dissolved solids in Liquid process Samples <https://www.nrel.gov/docs/gen/fy08/42621.pdf>
43. Jang, S. S., Shirai, Y., Uchida, M., & Wakisaka, M. (2012). Production of mono sugar from acid hydrolysis of seaweed. *African Journal of Biotechnology*, 11(8), 1953-1963.
44. Sappati, P. K., Nayak, B., VanWalsum, G. P., & Mulrey, O. T. (2018). Combined effects of seasonal variation and drying methods on the physicochemical properties and antioxidant activity of sugar kelp (*Saccharina latissima*). *Journal of Applied Phycology*, 1-22.
45. Merrill, A. L., & Watt, B. K. (1973). Energy value of Foods, basis and derivation. Agriculture research service. United States Department of Agriculture. Agriculture handbook, 74.
46. Sluiter, A., Hames, B., Ruiz, R., Scarlata, C., Sluiter, J., Templeton, D., & Crocker, D. (2008). Determination of structural carbohydrates and lignin in biomass. Laboratory analytical procedure, 1617, 1-16.
47. Tiwari, B. K., & Troy, D. J. (2015). Seaweed sustainability–food and nonfood applications. In *Seaweed Sustainability* (pp. 1-6).
48. CLENDENNING, K. A. (1962). Determination of fresh weight, solids, ash and equilibrium moisture in *Macrocystis pyrifera*. *Botanica Marina*, 4(3-4), 204-218.
49. Guschina, I. A., & Harwood, J. L. (2006). Lipids and lipid metabolism in eukaryotic algae. *Progress in lipid research*, 45(2), 160-186.

50. Jones, D. B. (1931). Factors for converting percentages of nitrogen in foods and feeds into percentages of proteins.
51. Angell, A. R., Mata, L., de Nys, R., & Paul, N. A. (2016). The protein content of seaweeds: a universal nitrogen-to-protein conversion factor of five. *Journal of Applied Phycology*, 28(1), 511-524.
52. Mian, A. J., & Percival, E. (1973). Carbohydrates of the brown seaweeds *himanthalia lorea*, *bifurcaria bifurcata*, and *Padina pavonia*: Part I. extraction and fractionation. *Carbohydrate Research*, 26(1), 133-146.
53. Schiener, P., Black, K. D., Stanley, M. S., & Green, D. H. (2015). The seasonal variation in the chemical composition of the kelp species *Laminaria digitata*, *Laminaria hyperborea*, *Saccharina latissima* and *Alaria esculenta*. *Journal of applied phycology*, 27(1), 363-373.
54. Stephen, A. M., & Phillips, G. O. (2016). *Food polysaccharides and their applications*. CRC press.
55. Edwards, D. M., Reed, R. H., Chudek, J. A., Foster, R., & Stewart, W. D. P. (1987). Organic solute accumulation in osmotically-stressed *Enteromorpha intestinalis*. *Marine Biology*, 95(4), 583-592.
56. Schiener, P., Black, K. D., Stanley, M. S., & Green, D. H. (2015). The seasonal variation in the chemical composition of the kelp species *Laminaria digitata*, *Laminaria hyperborea*, *Saccharina latissima* and *Alaria esculenta*. *Journal of applied phycology*, 27(1), 363-373.
57. Rioux, L. E., Turgeon, S. L., & Beaulieu, M. (2010). Structural characterization of laminaran and galactofucan extracted from the brown seaweed *Saccharina longicuris*. *Phytochemistry*, 71(13), 1586-1595.
58. Read, S. M., Currie, G., & Bacic, A. (1996). Analysis of the structural heterogeneity of laminarin by electrospray-ionisation-mass spectrometry. *Carbohydrate research*, 281(2), 187-201.
59. Li, C., & Zhao, Z. K. (2007). Efficient acid-catalyzed hydrolysis of cellulose in ionic liquid. *Advanced Synthesis & Catalysis*, 349(11-12), 1847-1850.
60. Heeres, H. J., Janssen, L. P. B. M., & Girisuta, B. (2006). A Kinetic Study on the Conversion of Glucose to Levulinic Acid.
61. Kemp, I. C. (2011). *Pinch analysis and process integration: a user guide on process integration for the efficient use of energy*. Elsevier.

62. Introduction to Pinch technology
<https://www.ou.edu/class/chedesign/adesign/Introduction%20to%20Pinch%20Technology-LinhoffMarch.pdf>
63. Pinch Analysis: For the efficient use of energy, water and hydrogen
https://www.nrcan.gc.ca/sites/www.nrcan.gc.ca/files/canmetenergy/pdf/fichier.php/codectec/En/2009-052/2009-052_PM-FAC_404-DEPLOI_e.pdf
64. Pinch Analysis: For the efficient use of energy, water and hydrogen
https://www.nrcan.gc.ca/sites/www.nrcan.gc.ca/files/canmetenergy/pdf/fichier.php/codectec/En/2009-052/2009-052_PM-FAC_404-DEPLOI_e.pdf
65. Pinch analysis: A tool for efficient use of Energy
<https://www.slideshare.net/arvindbjo/pinch-analysis-a-tool-for-efficient-use-of-energy>
66. Utilities and Energy Efficient Design
https://booksite.elsevier.com/samplechapters/9780080966595/Chapter_3.pdf
67. Sampath, G., Klein, S. J., Pendse, H. P., DeSisto, W. J., & Wheeler, M. C. (2018). Techno-economic analysis of thermal deoxygenation based biorefineries for the coproduction of fuels and chemicals. *Applied Energy*, 214, 16-23.
68. Bakošová, M., & Oravec, J. (2014). Robust model predictive control for heat exchanger network. *Applied Thermal Engineering*, 73(1), 924-930.
69. Zhang, H., Cui, G., Xiao, Y., & Chen, J. (2017). A novel simultaneous optimization model with efficient stream arrangement for heat exchanger network synthesis. *Applied Thermal Engineering*, 110, 1659-1673.
70. Bspang in heat transfer <http://www.cheresources.com/content/articles/heat-transfer/u-in-heat-exchangers>
71. Ulrich, G. D., & Vasudevan, P. T. (2006). How to estimate utility costs. *Chem. Eng*, 113(4), 66-69.
72. Peters, M. S., Timmerhaus, K. D., West, R. E., Timmerhaus, K., & West, R. (1968). *Plant design and economics for chemical engineers* (Vol. 4). New York: McGraw-Hill.
73. Costing and project evaluation <https://engineering.mu.edu.iq/wp-content/uploads/2017/01/Chapter-3>
74. Turton, R., Bailie, R. C., Whiting, W. B., & Shaeiwitz, J. A. (2008). *Analysis, synthesis and design of chemical processes*. Pearson Education.
75. Humbird, D., Davis, R., Tao, L., Kinchin, C., Hsu, D., Aden, A., ... & Sexton, D. (2011). *Process design and economics for biochemical conversion of lignocellulosic biomass to*

ethanol: dilute-acid pretreatment and enzymatic hydrolysis of corn stover (No. NREL/TP-5100-47764). National Renewable Energy Lab.(NREL), Golden, CO (United States).

76. Plant Design and Economics for chemical engineering
https://www.dioneoil.com/uploads/6/8/7/4/6874938/plant_design_and_economics_for_chemical_engineers.pdf
77. Sandler, H. J., & Luckiewicz, E. T. (1987). Practical process engineering: a working approach to plant design. McGraw-Hill

APPENDIX A MASS BALANCE CALCULATIONS

Cellulose and Laminarin content of Sugar kelp was calculated by assuming 11 wt% cellulose and 8 wt% Laminarin (56).

By considering 1 mol of cellulose converts into 1 mol of glucose

$$\textit{Theoretical yield of glucose (mmol)} = \textit{cellulose content (in mmol)} + \textit{Laminarin Content (in mmol)}$$

Equation 14 Theoretical yield of glucose (mmol)

$$\begin{aligned} \textit{\% of glucose yield (based on glucan content)} \\ = \frac{\textit{moles of glucose from HPLC}}{\textit{theoretical yield of glucose (in moles)}} * 100 \end{aligned}$$

Equation 15 % of glucose yield (based on glucan content)

$$\begin{aligned} \textit{\% of theoretical yield of levulinic acid (based on glucan content)} \\ = \frac{\textit{moles of levulinic acid produced}}{\textit{moles of glucose fed}} * 100 \end{aligned}$$

Equation 16 % of theoretical yield of levulinic acid (based on glucan content)

$$\begin{aligned} \textit{\% of levulinic acid yield (based on glucan content)} \\ = \frac{\textit{moles of levulinic acid from HPLC}}{\textit{theoretical yield of levulinic acid (in moles)}} * 100 \end{aligned}$$

Equation 17 % of levulinic acid yield (based on glucan content)

$$\textit{\% yield of levulinic acid (mol\%)} = \frac{\textit{moles of levulinic acid from HPLC}}{\textit{theoretical yield of levulinic acid (in moles)}} * 100$$

Equation 18 % yield of levulinic acid (mol%)

$$\textit{\% yield of levulinic acid (\%wt)} = \frac{\textit{the mass of levulinic acid from HPLC (mg)}}{\textit{total biomass fed (mg)}} * 100$$

Equation 19 % yield of levulinic acid (%wt)

APPENDIX B SUGAR ANALYSIS AND LEVULINIC ACID ANALYSIS OF SUGAR KELP

Table 19 Sugar Analysis Results of Sugar Kelp

	2% H ₂ SO ₄	4% H ₂ SO ₄	6% H ₂ SO ₄	8% H ₂ SO ₄	10% H ₂ SO ₄
60 min	3.64±0.16%	4.09±0.12%	4.45±0.12%	5.45±0.18%	4.33±0.69%
150 min	4.08±0.14%	4.52±0.05%	5.26±0.47%	6.05±0.22%	5.00±0.11%
240 min	6.0±0.12%	5.43±0.06%	5.38±0.05%	5.0±0.01 %	4.58±0.12%

(presented as wt %, by assuming total intel feedstock content 300 mg, at 121 ° C)

Table 20 Levulinic Acid as a Byproduct from Sugar Analysis of Sugar Kelp

	2% H ₂ SO ₄	4% H ₂ SO ₄	6% H ₂ SO ₄	8% H ₂ SO ₄	10% H ₂ SO ₄
60 min	N.D.	N.D.	N.D.	0.34±0.02%	0.31±0.05%
150 min	N.D.	N.D.	0.34±0.03%	0.86±0.04%	0.80±0.02%
240 min	N.D.	0.08±0.10%	0.61±0.41%	0.90±0.03 %	1.20±0.06%

(presented as wt %, by assuming total intel feedstock content 300 mg, at 121 ° C))

Table 21 Results of Levulinic acid from Two Stage Hydrolysis (with 4% H₂SO₄)

	150 °C		175 °C		200 °C	
	Yield of LA (% mol)	Yield of LA (% wt)	Yield of LA (% mol)	Yield of LA (% wt)	Yield of LA (% mol)	Yield of LA (% wt)
40 min	4.88	0.66	21.37	2.89	27.10	3.67
	6.09	0.7	20.81	2.82	28.42	3.85
	6.02	0.82	19.74	2.67	29.21	3.95
80 min	14.66	1.98	26.30	3.56	27.94	3.78
	16.29	2.21	29.01	3.93	29.70	4.02
	14.07	1.90	29.08	3.94	31.31	4.24
120 min	19.05	2.58	29.34	3.97	30.18	4.08
	18.80	2.54	29.26	3.96	30.06	4.07
	19.16	2.59	29.31	3.97	30.09	4.07

Table 22 Results of Levulinic acid from Two Stage Hydrolysis (with 6 wt% H₂SO₄)

	150 °C		175 °C		200 °C	
	Yield of LA (% mol)	Yield of LA (% wt)	Yield of LA (% mol)	Yield of LA (% wt)	Yield of LA (% mol)	Yield of LA (% wt)
40 min	13.11	1.77	42.54	5.76	48.76	6.60
	14.17	1.92	44.25	5.99	48.07	6.51
	14.60	1.98	44.28	5.99	49.27	6.67
80 min	29.34	3.97	44.22	5.98	49.73	6.73
	29.32	3.97	45.40	6.14	47.64	6.45
	29.22	3.95	45.48	6.15	47.06	6.37
120 min	33.37	4.52	44.54	6.03	32.51	4.40
	33.42	4.52	45.03	6.09	31.47	4.26
	33.48	4.53	44.94	6.08	31.97	4.33

Table 23 Results of Levulinic Acid from Two Stage Hydrolysis (with 8 wt% H₂SO₄)

	150 °C		175 °C		200 °C	
	Yield of LA (% mol)	Yield of LA (% wt)	Yield of LA (% mol)	Yield of LA (% wt)	Yield of LA (% mol)	Yield of LA (% wt)
40 min	35.08	4.75	58.79	7.96	53.07	7.18
	34.65	4.69	57.79	7.82	55.86	7.56
	34.60	4.68	58.70	7.94	56.23	7.61
80 min	51.66	6.99	61.75	8.36	48.78	6.60
	51.45	6.96	61.65	8.34	48.40	6.55
	51.52	6.97	61.75	8.36	49.29	6.67
120 min	57.16	7.74	60.07	8.13	60.92	8.24
	57.30	7.75	60.48	8.18	61.40	8.31
	57.51	7.78	60.07	8.13	48.51	6.56

Table 24 Results of Levulinic Acid from Three Stage Hydrolysis (with 4 wt% H₂SO₄)

	150 °C		175 °C		200 °C	
	Yield of LA (% mol)	Yield of LA (% wt)	Yield of LA (% mol)	Yield of LA (% wt)	Yield of LA (% mol)	Yield of LA (% wt)
40 min	6.76	0.92	23.13	3.13	23.54	3.19
	7.31	0.99	19.91	2.69	25.24	3.42
	6.59	0.89	22.62	3.06	25.89	3.50
80 min	14.58	1.97	24.72	3.35	27.43	3.71
	15.67	2.12	25.19	3.41	27.01	3.66
	12.94	1.75	22.81	3.09	26.58	3.60
120 min	19.96	2.70	25.99	3.52	25.41	3.44
	20.47	2.77	20.76	2.81	25.81	3.49
	15.58	2.11	26.31	3.56	24.28	3.29

Table 25 Results of Levulinic Acid from Three Stage Hydrolysis (with 6 wt% H₂SO₄)

	150 °C		175 °C		200 °C	
	Yield of LA (% mol)	Yield of LA (% wt)	Yield of LA (% mol)	Yield of LA (% wt)	Yield of LA (% mol)	Yield of LA (% wt)
40 min	9.06	1.23	22.75	3.08	28.19	3.82
	9.64	1.30	35.02	4.74	26.53	3.59
	8.38	1.13	24.17	3.27	26.30	3.56
80 min	26.07	3.53	36.94	5.00	30.12	4.08
	25.57	3.46	29.43	3.98	29.94	4.05
	26.02	3.52	41.25	5.58	27.47	3.72
120 min	18.66	2.53	31.59	4.28	30.10	4.07
	18.33	2.48	26.13	3.54	31.10	4.21
	19.21	2.60	30.10	4.07	27.91	3.78

Table 26 Results of Levulinic Acid from Three Stage Hydrolysis (with 8 wt% H₂SO₄)

	150 °C		175 °C		200 °C	
	Yield of LA (% mol)	Yield of LA (% wt)	Yield of LA (% mol)	Yield of LA (% wt)	Yield of LA (% mol)	Yield of LA (% wt)
40 min	20.72	2.80	36.90	4.99	52.63	7.12
	22.86	3.09	41.19	5.57	47.58	6.44
	23.88	3.23	35.16	4.76	39.32	5.32
80 min	27.98	3.79	40.75	5.52	39.19	5.30
	27.07	3.66	40.61	5.50	44.22	5.98
	25.24	3.42	37.40	5.06	43.77	5.92
120 min	29.96	4.05	35.69	4.83	42.59	5.76
	33.95	4.59	40.26	5.45	39.34	5.32
	35.76	4.84	38.32	5.19	40.96	5.54

APPENDIX C UTILITY COST OF THE PROCESS WITH AND WITHOUT ENGERY INTEGRATION

Table 27 Annual Cost of Utility with their Coefficients (Process with energy Integration)

Type of Utility	Mass Flow (kg/h)	a	b	Process module \$/kg or \$/m ³	Utility Price \$/year
High Pressure Steam	2665	3.54E-05	3.94E-03	0.03	65,901
Medium Pressure Steam	3623	2.68E-05	3.80E-03	0.03	815,050
Low Pressure Steam	83124	1.60E-06	3.46E-03	0.01	11,022,060
Cooling Water	188044	1.18E-04	3.00E-03	0.07	148,984

Table 28 Annual Cost of Utility with their Coefficients (Process w/o energy Integration)

Type of Utility	Mass Flow (kg/h)	a	b	Process module \$/kg or \$/m ³	Utility Price \$/year
High Pressure Steam	2665	3.54E-05	3.94E-03	0.029	660,528
Medium Pressure Steam	3624	2.68E-05	3.80E-03	0.03	479,375
Low Pressure Steam	203505	7.15E-07	3.46E-03	0.001	16,848,018
Cooling Water	380274	1.13E-04	3.00E-03	0.09	369,928

Table 29 HPAEC Results for Sugar Analysis Results of Sugar Kelp

	2% H ₂ SO ₄		4% H ₂ SO ₄		6% H ₂ SO ₄		8% H ₂ SO ₄		10% H ₂ SO ₄	
	(%mol)	(%wt)	(%mol)	(%wt)	(%mol)	(%wt)	(%mol)	(%wt)	(%mol)	(%wt)
60 min	15.33	3.23	30.36	6.41	46.86	9.90	69.62	14.70	82.93	17.50
150 min	15.73	3.31	31.53	6.65	40.82	9.61	63.01	13.30	64.47	13.60
240 min	13.92	2.93	27.59	5.82	42.59	9.00	51.32	10.11	59.02	10.26

(based on mol%, by assuming total glucan content 19%, at 121 ° C)

BIOGRAPHY

Maurvin G. Patel was born in Kadi, India on Sept 14, 1993. He graduated from Pandit Deendayal Petroleum University, India in May 2015 with Bachelor of Science in Chemical Engineering. He was working at Elixir Pharma as a graduate engineer trainee when he decided to continue his education in Master of Science in Chemical Engineering. He was accepted as graduate student at University of Maine Chemical Engineering in January 2016. He is a candidate for the Master of Science degree in Chemical Engineering from the University of Maine in May 2019.